

INVESTIGATION OF PLUTONIUM-BEARING
FUEL ELEMENTS FOR THE
PLUTONIUM RECYCLE TEST REACTOR (PRTR)

by

WENDELL JACK BAILEY

A THESIS

Submitted to

OREGON STATE COLLEGE

in partial fulfillment of
the requirements for the
degree of

MASTER OF SCIENCE

June 1961

APPROVED:

Redacted for Privacy

Assistant Professor of Mechanical Engineering

Redacted for Privacy

Head of Mechanical Engineering Department

Redacted for Privacy

Chairman of School Graduate Committee

Redacted for Privacy

Dean of Graduate School

Date thesis is presented June 10, 1960

Typed by Margaret Wood

TABLE OF CONTENTS

	<u>Page</u>
Introduction	1
Discussion	8
I. Irradiation Testing Program - Objectives	8
II. Plutonium Fuels - Problem Areas	9
III. Irradiation Tests - Fuel Element Design Considerations	14
IV. Specific Irradiation Tests	20
V. Fluid Flow, Heat Transfer, and Physics Calculations	36
VI. Fabrication of Test Specimens	58
VII. Zircaloy Tubing Problem	67
VIII. Evaluation Techniques	69
Results and Conclusions	70
Bibliography	99
Appendix	107
Notation	109

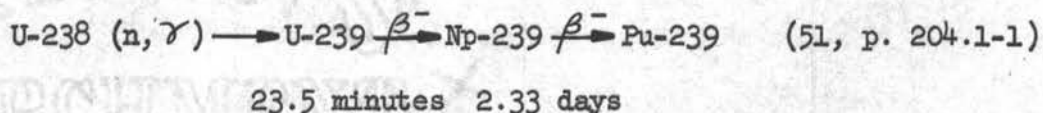
LIST OF FIGURES AND TABLES

<u>Figure Number</u>	<u>Page</u>	<u>Table Number</u>	<u>Page</u>
1	4	I	3
2	5	II	22
3	13	III	23
4	41	IV	24
5	49	V	26
6	71	VI	27
7	72	VII	29
8	73	VIII	30
9	74	IX	31
10	75	X	33
11	76	XI	35
12	77	XII	84
13	78	XIII	85
14	79		
15	80		
16	81		
17	82		
18	83		

INVESTIGATION OF PLUTONIUM-BEARING FUEL ELEMENTS
FOR THE PLUTONIUM RECYCLE TEST REACTOR (PRTR)

INTRODUCTION

Plutonium is produced by irradiating uranium fuel elements in a nuclear reactor. Part of the plutonium is fissioned in situ and functions as a stabilizer of reactivity. The remaining plutonium is retained by the fuel material. As a consequence, a significant amount of unburned plutonium is contained in discharged fuel elements (38, p. 1). If this plutonium in the spent fuel elements is recovered and charged into a reactor as an integral part of freshly prepared fuel elements, the process is termed "recycling." In general, a plutonium recycle reactor is considered to be one that generates all or a portion of its own plutonium requirements through the reaction:



The design of a nuclear power reactor may allow operation with natural uranium but there are definite gains to be made through the use of plutonium enrichment. One can increase the initial reactivity of a fuel element charge and thus prolong the useful life of the elements. One can also boost the amount of energy produced by the fuel loading. For a nuclear power reactor designed for operation with natural uranium as feed material, plutonium recycling provides a means by which a limited amount of enrichment can be obtained and used. It allows the reactor to function on a self-sustaining basis since plutonium may be separated from uranium by chemical means (10,

p. 461-462) or pyrometallurgical processing techniques (51, p. 204.1-1. This permits the power plant to be independent of diffusion plants which are presently required as a source for U-235 enrichment.

Although plutonium is present in five parts in 10^{12} in uranium ores, it is considered a synthetic element. The quantity of plutonium available is distinctly limited by the natural abundance of the fertile uranium isotope U-238, since plutonium cannot be obtained practically from any other isotope (40, vol. 3, p. 236).

Some selected nuclear properties of the metal plutonium may be seen in Table I. Inspection of the nuclear properties shown in Table I indicates that Pu-239 is strikingly different from U-235. An important point is the significant effect that moderator temperature has on the efficiency of plutonium utilization.

The investigation of the recycle concept has been undertaken by the Hanford Atomic Products Operation (HAPO) at Richland, Washington. An important part of the Plutonium Recycle Program is the Plutonium Recycle Test Reactor (PRTR), an experimental reactor, which is being constructed and is nearly completed (23, p. 816). The PRTR, shown in Figure 1, is cooled and moderated with heavy water and contains 85 vertical process tubes of the pressure-tube type. The fuel element (Figure 2) for the PRTR consists of an eight-foot long cluster of 19 rods. The 19 rods are held in a closely packed array by top and bottom brackets. The clusters are supported from the top of the vertical process tubes. The process tubes are arranged in an equilateral triangular eight-inch lattice and the coolant flow is upward.

Table I

EFFECT OF MODERATOR TEMPERATURE ON NUCLEAR
 PROPERTIES OF URANIUM-235 AND PLUTONIUM-239
 (36, p. 7, 9)

Average Moderator Temp., °C	Average Neutron Energy, (kT) ev	Fast Neutrons Produced Per Thermal Neutron Absorbed in:		$\bar{\sigma}_f$, Effective Fission Cross Section*, Barns	
		U-235	Pu-239	U-235	Pu-239
75	0.030	2.083	2.006	456	652
200	0.041	2.094	1.936	378	631
350	0.054	2.102	1.875	326	693
600	0.075	2.103	1.871	267	834

	$\bar{\sigma}_a$, Effective Absorption Cross Section*, Barns		Fraction of Atoms Fissioned		Available Fission Energy per Gram Destroyed, cal. x 10 ⁹	
	U-235	Pu-239	U-235	Pu-239	U-235	Pu-239
75	538	936	0.85	0.70	4.4	3.6
200	444	939	0.85	0.67	4.4	3.5
350	381	1060	0.85	0.65	4.4	3.4
600	312	1280	0.85	0.65	4.4	3.4

* $\bar{\sigma} = \sqrt{\pi}/2 \sigma_f(kT)$ where $\sigma_f(kT)$ is the monoenergetic cross section at the temperature, T, associated with the most probable energy of a Maxwell distribution, and f is the correction factor for departure from the "1/v" law.

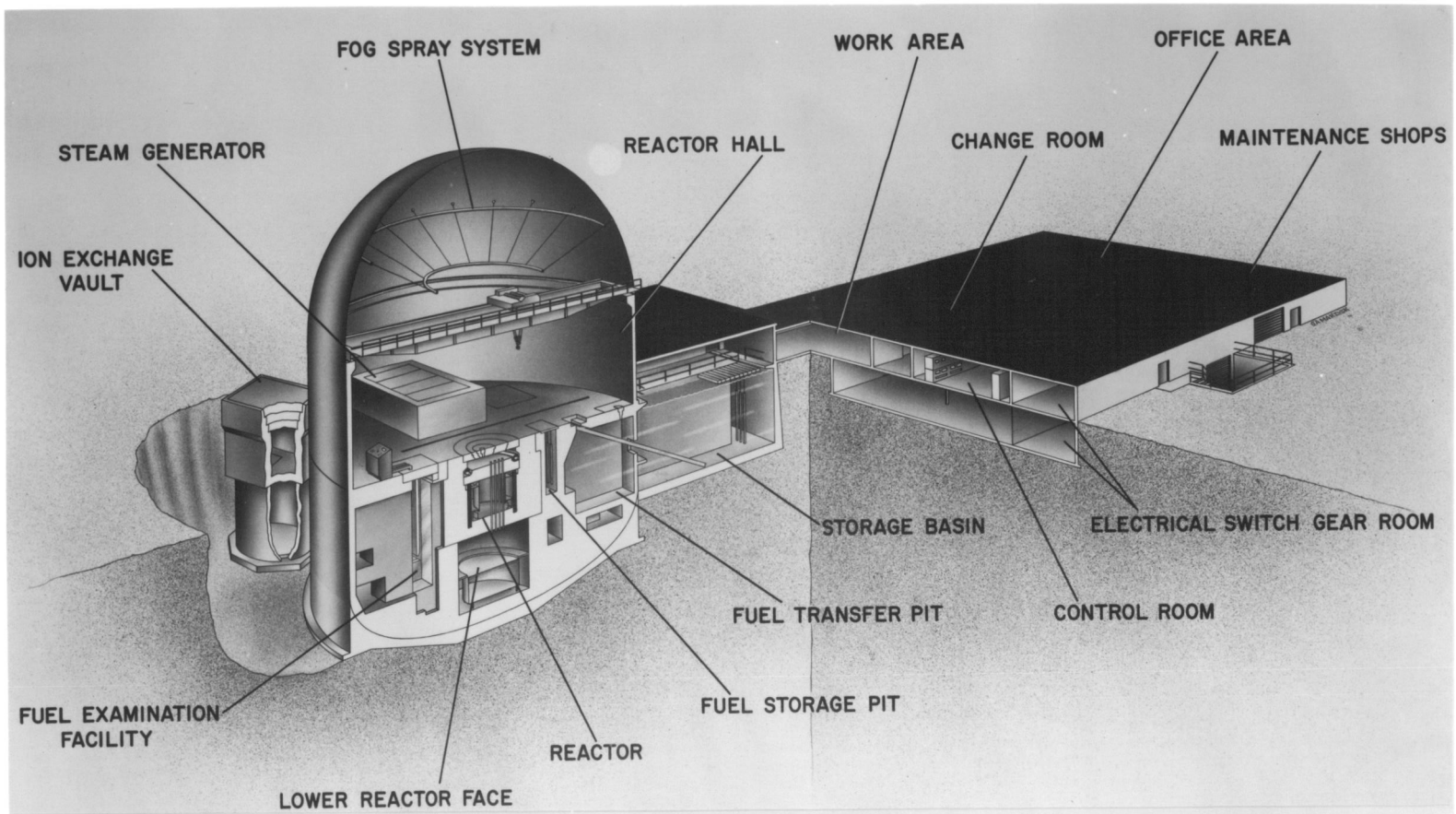


Figure 1
 Plutonium Recycle Test Reactor
 (PRTR)

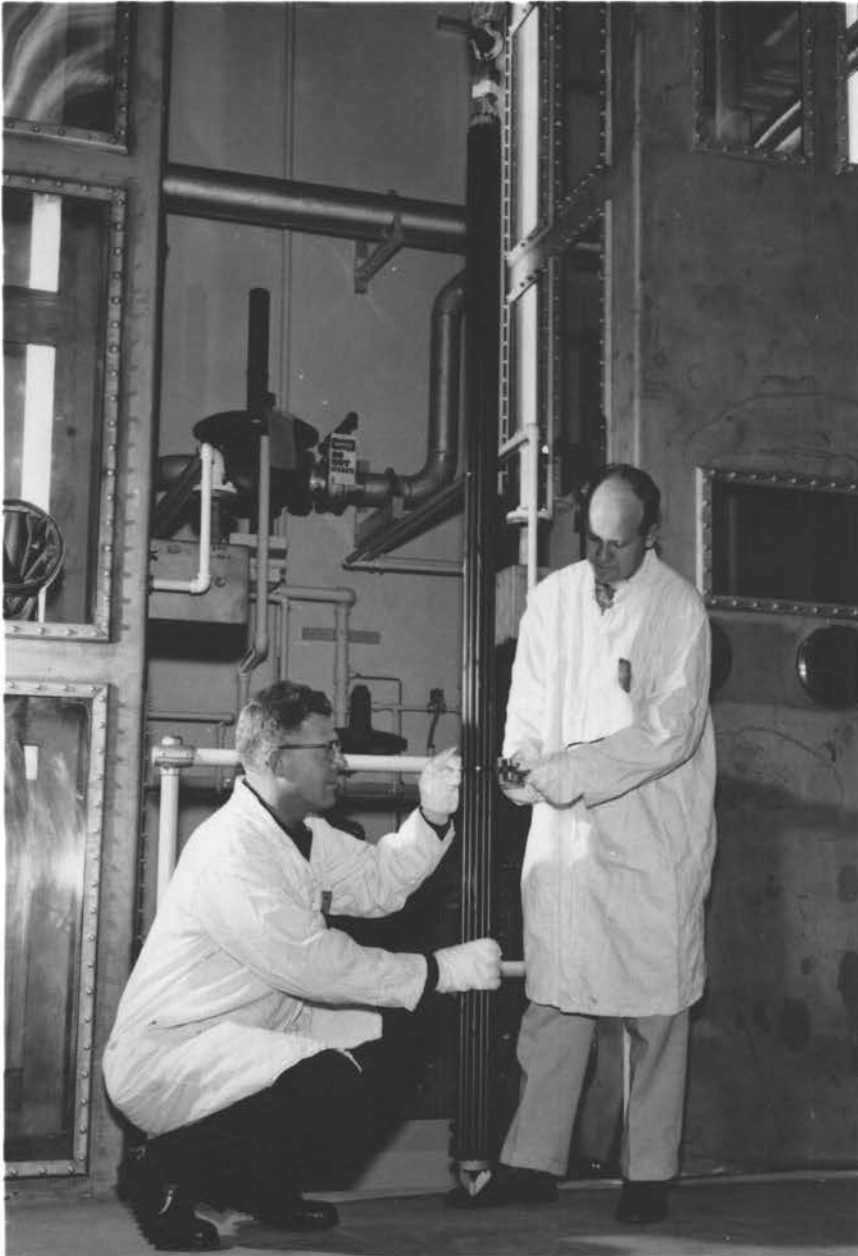


Figure 2
Zircaloy-Clad, Aluminum-Plutonium
Alloy Nineteen-Rod Cluster for the PRTR

Current planning for the PRTR calls for the insertion of 48-60 natural UO_2 fuel assemblies for the first fuel loading, plus 24-36 spike-enrichment assemblies which have cores of 1.8 weight percent plutonium (low exposure) alloyed with aluminum (4, p. 23). A spike-enrichment element is defined as one which utilizes a low concentration of plutonium in an inert carrier. The plutonium is composed primarily of the fissionable isotope Pu-239 with a low percentage of the nonfissionable isotope Pu-240 in the low exposure case and with 20 percent Pu-240 in the high exposure case. The number of spike-enrichment elements and their position will be adjusted in order to obtain the desired reactivity. Physics data will be collected as the initial fuel charge is irradiated and gradually the plutonium (low exposure), spike-enrichment elements will be replaced by plutonium (high exposure), spike-enrichment elements. The author is currently engaged in the fabrication of a number of fuel rods of the co-extruded, aluminum-clad, aluminum-plutonium alloy type for irradiation in order to provide the high exposure plutonium for these PRTR fuel clusters. Following the experiments with high-exposure plutonium spike-enrichment, mixed plutonium-uranium oxide assemblies will be inserted incrementally until the reactor is completely loaded with mixed oxide fuel and prepared for physics studies of a homogeneous fuel loading (35, p. 76). Exact composition of the fuel is not known as of this date, however, it is anticipated that the UO_2 (natural) will be combined with somewhat less than one atomic percent PuO_2 .

The aluminum-plutonium alloy was selected for the spike assemblies because more information was available on the fabrication and irradiation of this alloy and because of the extensive and satisfactory experience with aluminum-uranium alloy fuel elements. Selection of UO_2 for a fuel material was based on its compatibility with high temperature water, an important consideration in the event of a cladding rupture.

Zircaloy was the cladding material selected for the PRTR fuel clusters. The main points favoring Zircaloy over other types of cladding were its low thermal-neutron absorption cross section and its compatibility with the PRTR coolant system.

A key objective of the Plutonium Recycle Program is the development of plutonium-containing fuel materials which are readily fabricated and which display a high degree of performance. Of immediate interest and importance is the determination of the ex- and in-reactor characteristics of the fuel element materials selected for use in the PRTR.

This paper presents ten irradiation experiments with Al-Pu alloy, Al-Si-Pu alloy, and UO_2 - PuO_2 which have been performed under the direction of the author, a member of the Plutonium Fuels Development Operation, and as part of the PFDO Irradiation Testing Program. The author's particular role in the experimental work performed and reported in this thesis was to devise and carry out the irradiation tests described herein. One part of the author's work was to perform heat transfer and fluid flow calculations; make nuclear physics calcu-

lations, except for the P₃ - approximation type (40. vol.1, p. 381); design test fuel elements; specify reactor conditions; and prepare written irradiation test proposals. Another part was to specify compositions and obtain and inspect cladding and fuel core materials; direct or co-direct fabrication, ex-reactor testing, and inspection of fuel elements; and arrange for handling and irradiation of elements. The final part was to specify radiometallurgical examination work to be performed on irradiated elements and evaluate test results, draw conclusions, and make recommendations.

DISCUSSION

I. Irradiation Testing Program - Objectives

The investigation of plutonium-bearing fuel elements by the author and the Plutonium Fuels Development Operation has been directed toward several objectives. One is the selection of the exact composition of the fuel and cladding materials or alloys for the plutonium-containing fuel clusters required for immediate and near-future PRTR operation. A second objective is the determination of the design, fabrication method, quality control measures, and limitations for readily-prepared fuel elements in order to insure a high degree of performance under anticipated reactor operating conditions. Another objective is the investigation of potential plutonium-bearing fuels for the PRTR and for future reactors.

II. Plutonium Fuels - Problem Areas

One of the problem areas is the shortage of data on and irradiation experiments with aluminum-plutonium alloys in the composition range of interest. Little is known about the corrosion resistance of aluminum-plutonium alloys in high pressure and temperature water. A high-priority item was the selection of an alternate fuel material to replace the aluminum-plutonium alloy if it were found to be unsuitable.

The UO_2 - PuO_2 fuel material presents several problems. One is the acute lack of knowledge of the irradiation characteristics of a ceramic fuel. There is a scarcity of data on the fabrication and properties of the plutonium-uranium dioxide system. The form in which the PuO_2 is present in the ceramic fuel can markedly affect the dissolution of a UO_2 - PuO_2 pellet in acid, an important point for the separations process.

It is of major importance for the aluminum-plutonium alloy, UO_2 , and UO_2 - PuO_2 fuel elements to possess cladding with adequate strength and corrosion resistance. The cladding must provide as much protection as possible against a catastrophic failure. The behavior of operating PRTR fuel elements in the event of a cladding rupture is of vital concern when one considers that the defective element may be required to remain in operation in the reactor for a period as long as 24 hours after the detection of the rupture.

The presence of an undetected flaw in the cladding is serious for any fuel element either about to be irradiated or being irradiated. An extremely hazardous situation exists in the former case if the element contains plutonium, since there could conceivably be a sizeable spread of plutonium contamination in the storage area. In addition, if the element is charged into a reactor and appropriate precautionary measures are not taken, there exists the possibility of distributing plutonium contamination throughout the coolant system before sufficient activity has been accumulated to trip the reactor monitoring system.

To fully appreciate the seriousness of the hazard presented by uncontrolled plutonium, one needs to examine the characteristics of the synthetic element. Plutonium, a toxic metal, is one of the deadliest biological poisons known to man. Lack of adequate fuel fabrication equipment and facilities for the safe, continuous handling of plutonium has hindered more rapid development of plutonium fuels. The health hazard associated with plutonium is of prime importance since it is relatively independent of the amounts of plutonium involved (36, p. 5). Plutonium has a half-life of 24,300 years and though one generally regards it as only an alpha emitter, it is in the majority of instances a mixture of isotopes and as a result there is some associated low-energy gamma and X radiation. The alpha particles have a range of 3.68 centimeters in air and 45 microns

in tissue and have an energy of 5.15 million electron volts. The particles can inflict serious damage to the body tissue in the immediate vicinity surrounding the point of deposition of plutonium. Should plutonium enter the bloodstream it is rapidly and primarily deposited in and on the bone surfaces and the major damage in this event is the interference with the production of white corpuscles. The biological half life of plutonium in the body is approximately 100 years. The most important health hazard is the inhalation and consequent absorption through the lungs of plutonium and its compounds.

For plutonium fixed in bone matter the present maximum permissible body burden has been established at 0.04 microcuries or about 0.5 micrograms. At HAPO an employee is restricted from work with plutonium or a biologically similar isotope if his body burden has been determined to be in excess of one-fifth of the maximum allowable limit.

The stringent tolerances require exceedingly fine care in the fabrication and operation of plutonium handling facilities. A major reason for such meticulous care is the extreme mobility of plutonium, believed to be due to the formation of microscopic oxide particles.

Plutonium handling facilities are in general located in hoods or sealed glove boxes which are maintained at a slightly negative pressure. Manual operations are performed in hooded facilities by means of long rubber gloves which are securely

fastened and sealed to glove ports as shown in Figure 3. The exhaust from such facilities is filtered and care is taken to see that the concentration of plutonium in the exhaust does not exceed 2×10^{12} microcuries per cubic centimeter. It is of interest to note that the air concentration tolerance for plutonium is about one billionth of the value for chlorine which is considered industrially as a poisonous substance.

Actual manual handling times for plutonium metal or its alloys must be minimized in order to avoid excessive radiation exposure to the hands and body. Operations with high-exposure plutonium require shielding and manipulators to reduce the activity associated with the specimens to tolerable levels.

Plutonium has a very small critical mass, on the order of a few pounds (10, p. 466). If the mass is increased beyond the critical value, the associated radiation hazard from gamma rays and neutrons is tremendously increased. The more serious risk of an explosion may also be introduced. All proposed operations are reviewed by an experienced nuclear physicist before work is initiated.

Plutonium, especially in finely divided form, is pyrophoric and all forming operations performed on the material, particularly at elevated temperatures, involve serious hazards and must be conducted under controlled conditions. Plutonium metal and plutonium alloys may be subjected to all normal metal-working



Figure 3
Loading of Aluminum-Plutonium
Alloy Fuel Cores into Zircaloy-2 Tubes

processes. However, the physical and metallurgical properties of the particular material must be given careful consideration.

Some of the compounds and many of the alloys of plutonium are more pyrophoric than the pure metal. The UO_2 - PuO_2 and the aluminum-plutonium alloys are not pyrophoric.

III. Irradiation Tests - Fuel Element Design Considerations

It was decided to conduct the initial exploratory work on plutonium-bearing fuel elements with small capsules and clusters. It is planned to follow these initial tests with experiments in the PRTR with full-scale fuel elements. This approach to the fuel-investigation program agrees with the recommendations reported by other investigators (56, p. 538-539). They state that during the early stages of the investigation, the work is best conducted by irradiating a large number of small capsules so much information can be obtained and analyzed and yet keep the volume of irradiated material as low as possible. It was mutually agreed that this approach presents two inherent problems. One is that the reactor operating conditions of interest are difficult to duplicate. Secondly, it is extremely hard to predict what one may encounter with full-scale elements in a given reactor, based on the irradiation experience with capsules and small clusters in other reactors.

Since the PRTR fuel element consists of a cluster of 19 rods it was deemed desirable to select a short section of a single cluster rod as the tentative capsule design for the tests.

A typical cluster rod is composed of a solid, one-piece fuel core, one-half-inch in diameter by 88 inches long, and a Zircaloy tube which has an outside diameter of 9/16-inch and a wall thickness of 0.030 inch.

The Materials Testing Reactor (MTR) was selected for capsule experiments, since it offers high thermal-neutron fluxes, is able to accommodate a wide variety of experiments and conditions, and can effect high exposures in relatively short in-reactor periods. A number of capsules may be charged into a single coolant channel through the use of a stringer basket ("S" or "X" type). A capsule length of about two inches was established in order to provide a relatively uniform reactor environment for the specimen, to expedite positioning and testing in the reactor, and to limit the amount of plutonium present to as low a value as possible until actual test runs proved the design and materials were reliable. Even with this short section of fuel core, the thermal neutron flux gradients can be appreciable. In the case of one Al-1.65 Pu alloy test capsule (GEH-3-24-11), there was a 31 percent increase in the flux value over the two-inch length (65, p. 1).

For the cluster experiments, one of the high pressure and temperature loop facilities was selected. Two such facilities are the KER Loops at HAPO and the loops in the Engineering Test Reactor (ETR) at Arco, Idaho.

Heat transfer limitations in reactors severely restrict the use of fuel elements with high concentrations of plutonium and focus attention on the dilute plutonium alloys (up to 20 weight percent plutonium) as the prime fuel material source for reactor systems (32, p. 4) (73, p. 690-696). For the irradiation tests, two alloys, aluminum-plutonium and Al-12 weight percent Si-Pu, were selected and castings with 1.65-20 weight percent plutonium were prepared. In the early stages of design work on the PRTR it was indicated that the spike assemblies would contain 1.65 - 1.80 weight percent plutonium. In comparison to the aluminum-plutonium alloys, the Al-12 Si-Pu alloys are of interest because of the reported improvement in the corrosion behavior in high pressure and temperature water due to the silicon addition (14, p. 2). The superior casting properties, lower thermal-neutron cross section, and pyrometallurgical reprocessing advantages (76, HW-57343, p. 11-13) of the alloy are worthy of note. In addition, sounder cores are obtainable with this alloy in full-length, injection-cast, PRTR fuel rods (76, HW-55415, p. 11-13). Several disadvantages of the alloy are lower melting point and lower thermal conductivity values (70, p. 8). It is also a very difficult alloy to handle at a separations plant (72, p. 1-13).

Some of the properties of aluminum-plutonium and Al-12 Si-Pu alloys, such as the coefficient of linear expansion, density, hardness, ultimate and yield strength, elongation, reduction in

area, and extrusion constant, have been investigated and reported (70, p. 2-13) (34, p. 688-689).

At the time when the capsule and cluster irradiation tests were initiated, the only available method for preparing alloy fuel cores was to cast and machine rods. For the recent prototypical cluster experiments, wrought aluminum-plutonium alloy cores were employed. The cores were extruded from cast billets, processed through a rod straightener, and cut to exact length to form one-piece fuel cores for each cluster rod.

For the $\text{UO}_2\text{-PuO}_2$ fuel material investigation, high-density, sintered pellets and low-density, nonsintered pellets were tested. Two methods of obtaining the desired $\text{UO}_2\text{-PuO}_2$ solid solution in the pellets were explored. In one method, the ceramic fuel material is produced by the co-precipitation and calcination of Pu(OH)_4 and $(\text{NH}_4)_2\text{U}_2\text{O}_7$ from hot ammonium hydroxide (17, p. 7). Recent work by Chikalla (17, p. 4-7) (18, p. 3-4) (19, p. 1-2) demonstrates that solid solutions may also be prepared by sintering mixtures of UO_2 and PuO_2 powders in hydrogen at 1600 C. It was stated that formation of the single, face-centered cubic phase was verified by x-ray diffraction techniques and determination of the crystal lattice parameters. The solid solution formed by sintering in hydrogen is being evaluated for several reasons: (1) it eliminates the necessity of performing the chemical processing steps, (2) the UO_2 and PuO_2 are readily available, and (3) the dissolution rate

in acid of the material is comparable to that of the co-precipitated material. The dissolution rate of a physical mixture of $\text{UO}_2\text{-PuO}_2$ is markedly lower than that for either of the types of solid solutions.

The sintered $\text{UO}_2\text{-PuO}_2$ pellets with densities of 85 - 95 percent of the theoretical value are of particular interest because of the favorable irradiation performance which has been reported (16, p. 1-33) (43, p. 1-22). The low-density (65 - 70 percent of the theoretical value) pellets are being investigated because of the ease of fabrication and the distinct possibility of obtaining solid solution formation by having in situ sintering occur during irradiation (11, p. 2).

For the irradiation test capsules, $\text{UO}_2\text{-PuO}_2$ pellets containing 0.0259 - 7.45 atomic percent PuO_2 and having densities on the order of 65 and 90 percent of the theoretical value were prepared by Chikalla (76, HW-60996, p. 15). For the high-density and the low-density pellets, the PuO_2 concentrations were established by computer calculations (76, HW-59365, p. 7,9) so that the power generation values would be equivalent to that of Al-1.8, 5, 10, 15, and 20 plutonium alloy cores of the same diameter under similar reactor conditions.

The cladding for the different test specimens was obtained in three ways: (1) by machining jacketing parts from solid Zircaloy-2 bar, (2) by using Zircaloy-3 extruded tubing and Zircaloy-2 end fittings, and (3) by employing Zircaloy-2 end

caps and extruded tubing. The all-machined parts were made during the period when extruded tubing of the appropriate size was not available. At one time Zircaloy-3 was considered as a possible PRTR cladding material and a limited amount was purchased for use on experimental elements. In comparison to Zircaloy-2, the Zircaloy-3 was reported to be as good or better from the standpoint of corrosion (44, p. 6-8) but displayed less favorable mechanical properties (26, p. 5) (67, p. 26-38). It has been found that Zircaloy-3 is prone to stringer-type corrosion in the high pressure and temperature water (39, p. 39-47). It was subsequently decided to specify Zircaloy-2 for the initial PRTR fuel element charge. All of the prototypical fuel clusters for irradiation testing have been clad with extruded, Zircaloy-2 tubing.

The design of all of the capsule and cluster experiments was based on duplicating as nearly as possible one or more of the reactor operating conditions anticipated for PRTR fuel elements. A number of the more pertinent conditions for the PRTR are shown below:

(a) Coolant Temperature	478 F - 545 F
(b) Coolant Pressure	1050 psig
(c) Thermal Neutron Flux	$0.5 - 1.2 \times 10^{14}$ nv
(d) Fuel Rod Heat Flux	252,000 - 400,000 Btu/(hr) (sq ft)
(e) Fuel Rod Specific Power	11 - 17 kw/ft

(f) Exposures, Al-Pu Alloy	50 percent burnup of fissionable material, maximum
UO_2, UO_2-PuO_2	5000 Mwd/t
(g) Fuel Temperatures,	
Al-Pu Alloy; UO_2, UO_2-PuO_2	748 F maximum; 2660 F maximum
(h) Power, Maximum	1200 kw/tube
(i) Reactor Power Output	1300 Mwd/month

In the fabrication of the experimental capsules and clusters, an effort was made to use a technique which would be applicable to full-scale PRTR elements. It was considered of major importance to perfect a means of assembling fuel elements with a minimum of external plutonium contamination. The determination of quality control measures to insure high integrity fuel cladding on experimental capsules and clusters and on full-scale PRTR fuel elements was known to be a significant item.

IV. Specific Irradiation Tests

The initial capsule experiment, GEH-3-24, involved four specimens (65, p. 1-7) (76, HW-51854, p. 5-20). All were clad in Zircaloy-2 jacketing components which were made by machining bar stock. Two capsules contained Al-1.65 Pu alloy fuel cores and two had Al-12 Si-1.65 Pu alloy cores. The primary purpose in this test was to obtain reactor experience with nonbonded cast fuel cores and to evaluate the performance of the alloy samples. It was originally planned to have the capsules of each type subjected to 25 and 50 percent burnups by fission of

the plutonium atoms. A summary of the capsule data and actual irradiation conditions are shown in Table II. Typical heat transfer, fluid flow, and physics calculations for alloy and oxide tests are shown below along with details of the fabrication techniques.

The second experiment, GEH-14-23, 24, 25, and 26, was similar to the initial capsule test and the specimens were prepared in the same manner (64, p. 1-2) (76, HW-61994, p. 7). The objective of the test was to verify and supplement the data and experience obtained from the GEH-3-24 capsules and to establish the irradiation behavior of the alloys at higher burnup values (60 - 100 percent) for the plutonium atoms. The actual irradiation conditions and the capsule data may be seen in Table III.

The third set of capsules, GEH-14-5 through 12, was fabricated with cast fuel cores of aluminum-plutonium and Al-12 Si-Pu alloys containing 5, 10, 15, and 20 weight percent plutonium (58, p. 1-7) (76, HW-57342, p. 7). The cladding consisted of Zircaloy-3 tubing and Zircaloy-2 end caps. The prime purpose of this experiment was to determine the irradiation behavior of aluminum-plutonium and Al-12 Si-Pu alloys containing higher plutonium concentrations and to provide material for radiometallurgical examination and reprocessing and separations studies. Actual irradiation conditions for and information on the capsules are shown in Table IV.

Table II - Results from GEH-3-24 (Capsules 5, 8, 9, and 11)
Irradiation Test

No.	Fuel Core Alloy, w/o	Neutron Flux, ϕ_{cs} ; $n\nu \times 10^{14}$	Exposure, ($\phi_{cs}t$); $nvt \times 10^{20}$	(Fissions per cu cm) $\times 10^{18}$	Thermal Cycles, No.
9	Al-1.65 Pu	3.3	7.00	47	37(8)
11	Al-1.65 Pu	1.1	2.39	23	29(6)
5	Al-12 Si-1.65 Pu	1.6	1.80	17	13(3)
8	Al-12 Si-1.65 Pu	3.4	7.63	50	53(11)

No.	Fractional Burnup of Pu Atoms, %	Calculated Core Temp., % Range	Specific Power, kw/ (ft of rod)	Heat Flux, 10^6 Btu/ (hr)(sq ft)
9	43	845(706-984)	42	0.98
11	20	360(313-405)	14	0.33
5	15	553(470-636)	15	0.35
8	45	900(752-1050)	43	1.0

No.	Core $\Delta V/V$; By ΔD , ΔL ; %	$10^{-22} \Delta V/V$ (Fissions/ cu cm)	Length Change, (in.) $\times 10^{-3}$	
	Range	Range	Core	Clad
9	0.38(0-0.88)	0.81(0.2-4)	4.0	5.1
11	1.1(0.57-1.6)	4.8(2.0-8.9)	-0.5	11.6
5	0.81(0.31-1.3)	4.8(1.5-10)	3.1	1.7
8	0.76(0.26-1.3)	1.5(0.42-3.4)	3.0	7.5

Note - See Appendix for estimate of precision of tabular values.

ϕ_{cs} = thermal neutron flux at core surface. 37(8) means 37 reactor power reductions, of which (8) were shutdowns.

Table III - Results from GEH-14-23, 24, 25, and 26 Irradiation Test

No.	Fuel Core Alloy, w/o	Neutron Flux, ϕ_{cs} ; $nv \times 10^{14}$	Exposure, (ϕ_{cst}); $nvt \times 10^{20}$	(Fissions per cu cm) $\times 10^{18}$	Thermal Cycles, No.
23	Al-1.65 Pu	2.7	10.8	61	38(8)
24	Al-1.65 Pu	2.3	9.02	55	38(8)
25	Al-12 Si-1.65 Pu	1.4	8.37	53	42(10)
26	Al-12 Si-1.65 Pu	2.7	14.2	65	42(10)

No.	Fractional Burnup of Pu Atoms, %	Calculated Core Temp., °F Range	Specific Power, kw/(ft of rod)	Heat Flux, 10^6 Btu/(hr)(sq ft)
23	53	710(599-825)	35	0.81
24	49	625(526-720)	29	0.68
25	47	440(377-501)	18	0.41
26	58	740(621-859)	35	0.81

No.	Core $\Delta V/V$; By $\Delta D, \Delta L$; % Range	$10^{-22} \Delta V/V$ (Fissions/cu cm) Range	Length Change, (in.) $\times 10^{-3}$ Core Clad	
23	0.23(0-0.73)	0.38(0-1.6)	0.5	4.3
24	0.10(0-0.60)	0.18(0-1.4)	2.0	4.2
25	0.68(0.18-1.2)	1.3(0.28-2.9)	2.0	3.6
26	1.2(0.70-1.7)	1.9(0.88-3.4)	4.0	-8.2

Note - See Appendix for estimate of precision of tabular values.

ϕ_{cs} = thermal neutron flux at core surface. 38(8) means 38 reactor power reductions, of which (8) were shutdowns.

Table IV - Results from GEH-14-5 Through 12 Irradiation Test

No.	Fuel Core Alloy, w/o	Neutron Flux, ϕ_{cs} ; $nv \times 10^{14}$	Exposure, (ϕ_{cst}); $nvt \times 10^{20}$	(Fissions per cu cm) $\times 10^{18}$	Thermal Cycles, No.
8	Al-5 Pu	1.2	3.25	80	56(12)
5	Al-10 Pu	0.37	0.788	45	29(8)
9	Al-15 Pu	0.23	0.966	75	66(14)
10	Al-20 Pu	0.15	0.465	47	43(10)
6	Al-12 Si-5 Pu	0.99	1.39	39	56(12)
11	Al-12 Si-10 Pu	0.29	0.627	35	29(8)
7	Al-12 Si-15 Pu	0.21	0.798	69	66(14)
12	Al-12 Si-20 Pu	0.12	0.372	39	43(10)

No.	Fractional Burnup of Pu Atoms, %	Calculated Core Temp., $^{\circ}F$	Specific Power, kw/ (ft of rod)	Heat Flux, 10^6 Btu/ (hr)(sq ft)
		Range		
8	24	970(808-1122)	49	1.2
5	6.4	720(603-841)	35	0.80
9	7.1	750(632-874)	37	0.86
10	3.1	760(640-886)	38	0.87
6	12	850(712-992)	41	0.94
11	5.2	610(517-705)	27	0.63
7	5.9	730(611-845)	34	0.79
12	2.5	730(554-760)	30	0.70

No.	Density Decrease, %	Core $\Delta V/V$; By $\Delta D, \Delta L$; %	$\left(\frac{10^{-22} \Delta V/V}{\text{Fissions/cu cm}} \right)$		Length Change (in.) $\times 10^{-3}$	
			By Density	By $\Delta D, \Delta L$	Core	Clad
			Range	Range		
8	0.46	2.0	0.58(0.25-1.1)	2.5(1.5-4.1)	11.3	5.3
5	0.37	0.58	0.83(0.27-1.7)	1.3(0.15-3.1)	11.6	5.5
9	0.33	0.88	0.44(0.12-0.96)	1.2(0.41-1.2)	9.0	17.0
10	0.16	1.8	0.34(0-1.1)	3.8(2.3-6.4)	11.2	0
6	0.58	0.99	1.5(0.75-2.7)	2.5(1.0-5.0)	0.8	17.8
11	0	0.78	0(0-0.56)	2.2(0.65-4.8)	0.6	16.0
7	0.72	0.68	1.1(0.59-1.8)	0.98(0.21-2.2)	-1.2	-1.5
12	0.22	--	0.56(0-1.5)	--	--	7.5

Note - See Appendix for estimate of precision of tabular values.

ϕ_{cs} = thermal neutron flux at core surface. 56(12) means 56 reactor power reductions, of which (12) were shutdown.

The fourth experiment with a set of capsules, GEH-14-42 through 49, was an exact duplicate of the third experiment with the exception that the test called for twice the exposure (59, p. 1-4) (76, HW-61994, p. 7). Actual conditions for the irradiation test and capsule data are shown in Table V.

The fifth set of capsules, GEH-14-19 and 20, contained UO_2 - PuO_2 fuel cores and was clad in machined, Zircaloy-2 jacketing components (60, p. 1-11) (76, HW-57343, p. 7). The two capsules each held two, sintered, high-density UO_2 - PuO_2 pellets. The pellets contained 0.0259 atomic percent PuO_2 and were fabricated by combining UO_2 - PuO_2 mixed-crystal-oxide ($UO_2:PuO_2::5:1$) and natural UO_2 . This experiment was conducted in order to gain reactor experience with the Zircaloy-clad high-density oxide pellets and to evaluate this future PRTR fuel material. The actual irradiation conditions and capsule data are presented in Table VI.

The sixth experiment was performed with a set of specimens, GEH-14-21 and 22, which had low-density, nonsintered, UO_2 - PuO_2 pellets and machined, Zircaloy-2 cladding (63, p. 1-10) (76, HW-57343, p. 9). The capsules each contained three pellets. All pellets had the same composition, 0.0259 atomic percent PuO_2 , and were produced by using the same starting materials that were employed for the GEH-14-19 and 20 capsules. The test had as its objective the evaluation of the irradiation behavior of the low-density oxide fuel with particular reference

Table V - Results from GEH-14-42 Through 49 Irradiation Test

No.	Fuel Core Alloy, w/o	Neutron Flux, ϕ_{cs} ; $\text{nv} \times 10^{14}$	Exposure (ϕ_{cst}); $\text{nvt} \times 10^{20}$	(Fissions Per cu cm) $\times 10^{18}$	Thermal Cycles, No.
45	Al-5 Pu	0.83	3.22	80	75(15)
43	Al-10 Pu	0.41	1.64	89	62(13)
44	Al-15 Pu	0.22	1.34	105	101(22)
42	Al-20 Pu	0.18	0.741	77	62(13)
48	Al-12 Si-5 Pu	0.83	3.24	79	75(15)
47	Al-12 Si-10 Pu	0.44	1.79	94	62(13)
46	Al-12 Si-15 Pu	0.22	0.664	56	43(10)
49	Al-12 Si-20 Pu	0.16	0.809	83	85(17)

No.	Fractional Burnup of Pu Atoms, %	Calculated Core Temp., $^{\circ}\text{F}$	Specific Power, kw/(ft of rod)	Heat Flux, 10^6 Btu/(hr)(sq ft)
		Range		
45	24	710(594-818)	34	0.79
43	13	670(567-779)	38	0.89
44	9.6	730(610-842)	35	0.82
42	5.0	890(744-1040)	45	1.0
48	24	730(616-850)	34	0.79
47	14	790(663-919)	37	0.86
46	5.0	760(636-880)	35	0.84
49	5.4	890(744-1038)	40	0.89

No.	Density Decrease, %	Core $\Delta V/V$; $10^{-22} \Delta V/V$		Length Change, (in.) $\times 10^{-3}$		
		By $\Delta D, \Delta L$, %	By Density	By $\Delta D, \Delta L$	Core	Clad
			Range	Range		
45	0.036	0.13	0.045(0-0.42)	0.16(0-1.0)	-1.0	-6.0
43	0.067	0.37	0.075(0-0.42)	0.42(0-1.3)	+0.1	+2.0
44	0	0.25	0(0-0.33)	0.24(0-0.93)	+0.6	-3.0
42	0.061	0.18	0.079(0-0.48)	0.23(0-1.2)	+3.5	-2.6
48	0.39	0.99	0.50(0.18-1.0)	1.3(0.51-1.3)	+1.1	-8.2
47	1.5	0.35	1.6(1.1-2.4)	0.37(0-1.2)	+3.4	+1.1
46	--	--	--	--	--	--
49	--	--	--	--	--	-6.0

Note - See Appendix for estimate of precision of tabular values. ϕ_{cs} = thermal neutron flux at core surface. 75(15) means 75 reactor power reductions, of which (15) were shutdowns. Core-clad bonding observed on No. 49.

Table VI - Results from GEH-14-19 and 20 Irradiation Test

Capsule Number	19	20
UO ₂ -PuO ₂ , a/o PuO ₂	0.0259	0.0259
Percent of Theoretical Density	91	90
Thermal Neutron Flux, ϕ_{CS} ; nv x 10 ¹⁴	1.5	1.5
Exposure, (ϕ_{CS} t); nvt x 10 ²⁰	4.03	4.03
Specific Power, kw/ft	15	15
Heat Flux, 10 ⁶ Btu/(hr)(sq ft)	0.35	0.34
10 ¹⁸ Fissions/cu cm	28	28
Fissionable Atoms Fissioned, %:		
Pu-239	29	29
U-235	19	19
Fission Gas Released, Kr-85; %	~3	
Thermal Cycles	30(6)	30(6)

Note - See Appendix for estimate of precision of tabular values. ϕ_{CS} = flux at fuel core surface.

30(6) means 30 reactor power reductions, of which (6) were shutdowns.

to in-reactor sintering and fission-gas release. Table VII contains the actual irradiation conditions and data for the specimens.

The seventh capsule experiment, GEH-14-82 through 91, was performed with sintered, high-density, $\text{UO}_2\text{-PuO}_2$ pellets clad with machined Zircaloy-2 components (57, p. 1-12) (76, HW-57343, p. 9). The pellets ranged in composition from 0.0259 to 5.67 atomic percent PuO_2 . Each capsule contained three pellets. The fuel materials were prepared by using a mechanical mixture of UO_2 and PuO_2 . This experiment was carried out to supplement the fifth test, GEH-14-19 and 20, and to obtain data on $\text{UO}_2\text{-PuO}_2$ mixtures. The capsule data and actual irradiation conditions are shown in Table VIII.

The eighth set of capsules, GEH-14-65 through 74, had low-density, nonsintered, $\text{UO}_2\text{-PuO}_2$ pellets jacketed in machined, Zircaloy-2 parts and possessed fuel cores ranging in PuO_2 concentration from 0.187 to 7.45 atomic percent (61, p. 1-9) (76, HW-57343, p. 9). As in the case of the seventh capsule set, these specimens were prepared by using a mechanical mixture of UO_2 and PuO_2 . In this test, it was desired to collect information on the reactor performance of low-density pellets, in particular the in-reactor sintering and the release of fission gas, and to supplement the results from the sixth experiment, GEH-14-21 and 22. Actual irradiation conditions and sample data are located in Table IX.

Table VII - Results from GEH-14-21 and 22 Irradiation Test

Capsule Number	21	22
UO ₂ -PuO ₂ , a/o PuO ₂	0.0259	0.0259
Percent of Theoretical Density	65	65
Thermal Neutron Flux, ϕ_{CS} ; nv x 10 ¹⁴	0.94	1.4
Exposure, ($\phi_{CS}t$); nvt x 10 ²⁰	2.88	10.8
Specific Power, kw/ft	6.8	10
Heat Flux, 10 ⁶ Btu/(hr)(sq ft)	0.16	0.23
10 ¹⁸ Fissions/cu cm	14	42
Fissionable Atoms Fissioned, %:		
Pu-239	22	52
U-235	14	42
Fission Gas Released, Kr-85; %	~22	
Thermal Cycles	47(9)	98(18)

Note - See Appendix for estimate of precision of tabular values. ϕ_{CS} = flux at fuel core surface.

47(9) means 47 reactor power reductions, of which (9) were shutdowns.

Table VIII - Results from GEH-14-82 Through 91 Irradiation Test

Capsule Number	90	91	82	83	84	85	86	87	88	89*
UO ₂ -PuO ₂ , a/o PuO ₂	0.0259	0.0259	1.02	1.02	2.57	2.57	4.13	4.13	5.67	5.67
Percent of Theoretical Density	90	90	93	93	93	91	91	91	91	91
Thermal Neutron Flux, ϕ_{CS} : nv x 10 ¹⁴	1.1	1.4	0.58	0.60	0.28	0.16	0.14	0.14	0.13	0.13
Exposure, ($\phi_{CS}t$); nvt x 10 ²⁰	3.22	15.8	5.12	1.22	0.588	2.14	1.63	0.438	0.222	1.69
Specific Power, kw/ft	11	14	18	18	16	9.0	11	11	12	12
Heat Flux 10 ⁶ Btu/(hr)(sq ft)	0.25	0.32	0.41	0.42	0.36	0.21	0.25	0.25	0.27	0.27
10 ¹⁸ Fissions/cu cm	23	77	95	28	26	85	91	26	16	114
Fissionable Atoms Fissioned, %:										
Pu-239	24	60	33	10	5	15	11	3	1	10
U-235	16	53	23	6	3	9	7	2	1	6
Kr-85 Released, %				<0.01				<0.1		<0.01
Thermal Cycles	54(11)	122(24)	110(23)	48(14)	33(8)	95(17)	116(20)	54(11)	38(9)	64(13)

* This specimen ruptured when later inadvertently placed in flux 11 times higher than design value.

Note - See Appendix for estimate of precision of tabular values. ϕ_{CS} = flux at fuel core surface. 54(11) means 54 reactor power reductions, of which (11) were shutdowns.

Table VII - Results from GEH-14-65 through 74 Irradiation Test

Capsule Number	65	66	67	68	69	70	71	72	73	74
UO ₂ -PuO ₂ , a/o PuO ₂	0.187	0.187	1.46	1.46	3.47	3.47	5.46	5.46	7.45	7.45
Percent of Theoretical Density	65	65	66	65	64	64	63	63	63	63
Thermal Neutron Flux, ϕ_{CS} ; nv x 10 ¹⁴	0.99	0.99	0.35	0.35	0.17	0.16	0.11	0.12	0.084	0.070
Exposure, (ϕ_{CS} t); nvt x 10 ²⁰	6.00	8.93	1.13	4.03	1.91	0.528	1.04	0.39	0.970	0.272
Specific Power, kw/ft	9.6	9.6	9.9	9.8	8.8	8.2	7.6	8.3	6.9	5.8
Heat Flux, 10 ⁶ Btu/(hr)(sq ft)	0.22	0.22	0.23	0.23	0.20	0.19	0.17	0.19	0.16	0.13
10 ¹⁸ Fissions/cu cm	36	48	24	72	71	21	54	21	61	18
Fissionable Atoms Fissioned, %:										
Pu-239	38	48	9.4	28	14	4.2	7.2	2.8	3.6	1.8
U-235	27	37	5.6	18	8.5	2.4	4.3	1.6	6.1	1.0
Fission Gas Released, Kr-85; % ~ 21			~0.14			~2		~8		~0.2
Thermal Cycles	65(10)	127(19)	49(8)	111(17)	111(17)	49(8)	111(17)	49(8)	111(17)	54(6)

Note -- See Appendix for estimate of precision of tabular values. ϕ_{CS} = flux at fuel core surface.

65(10) means 65 reactor power reductions of which (10) were shutdowns.

The ninth test, IP 186A, was the irradiation of a four-rod cluster element in a high pressure and temperature loop facility at HAPO (8, p. 1-6). The primary objective of this test was to obtain irradiation experience with a cluster element in near-PRTR coolant conditions. The cluster was constructed with Al-8 Pu alloy and Al-12 Si-8 Pu alloy cores and Zircaloy-3 tubing and Zircaloy-2 end caps. The individual rods were held in position by stainless steel end fixtures. The fluid flow and heat transfer data and details of the element fabrication and test conditions have been reported (76, HW-57343, p. 9) (7, p. 1-9) (6, p. 1-21). In general, the calculations were very similar to the ones shown below for the alloy capsules. Physics and reactor data were obtained and reported by Kratzer (45, p. 1-27). Flow tests were made and documented by Doman (24, p. 1-10). A summary of cluster data and actual irradiation conditions in KER-Loop 3 is available in Table X.

The tenth experiment, IP 226A, was conducted with a prototypical, seven-rod cluster which was fabricated with extruded, Al-1.8 Pu alloy fuel cores, Zircaloy-2 tubing and end caps, stainless steel end fixtures, and quick-disconnect fittings (76, HW-60996, P. 8-10) (6, p. 1-21). The cluster element duplicates as nearly as possible the appearance and construction of the center rod and six-rod ring of one of the latest designs for the aluminum-plutonium alloy, 19-rod,

Table X - Results from IP 186A, Four-Rod Cluster Irradiation Test

Rod No.	Fuel Core Alloy, w/o	Core Volume Change % Range	Initial ΔD , (in.) $\times 10^{-3}$,		Length Change, (in.) $\times 10^{-3}$	
			Avg.	Range	Core	Clad
1T	Al-8 Pu	0 (0-0.46)	2.0	1.6-2.4 ¹⁰	-10.1] 6.0
1B	Al-8 Pu	0.17(0-0.81)	3.5	3.4-3.5	- 9.0	
7	Al-8 Pu	0 (0-0.68)	4.6	3.8-5.4	7.8	1.0
8T	Al-8 Pu] 0.25*(0-0.67)	2.9	1.7-4.0] -29.5] 6.0
8B	Al-8 Pu		3.9	3.7-4.1		
11T	Al-12 Si-8 Pu	*	3.4	3.3-3.4] -25.6] 30.0
11B	Al-12 Si-8 Pu	*	4.5	4.3-4.6		

General Information**

Exposure, Estimated	3.0 $\times 10^{20}$ nvt
Rod Warp	None visually detected
Coolant Conditions	1500-1600 psig, 185-210°C, pH6
Cladding, Tubing	Zircaloy-III, extruded
End Caps	Zircaloy-II, machined
Rod End Fixtures	Stainless steel (304 L alloy) clips and bands
Rod Size, OD	0.563 in. (end caps, 0.680 in.)
Length	10 in.
Tube Wall	0.030 in.
Core OD	0.500 in.
Core Length	4 in., except No. 7 (8 in.)
Assembly Method	Slip fit (no lubricant used)
Rod Spacing (to nearest rod)	0.75 in., center-to-center
Cluster Size, OD	2.08 in. (at ends)
Length	10 in.
Total Pu Content	24.25 gm

* Cores 8T and 8B diffusion bonded at ends in reactor.
Cores 11T and 11B damaged during dejacketing step.

** See Appendix for estimate of precision of tabular values.

PRTR fuel element cluster. The prime purpose of this test was to acquire in-reactor experience with a prototypical element in near-PRTR coolant conditions. All rods in the six-rod ring are spirally wrapped with Zircaloy-2 wire. This experiment represents the first in-reactor usage of the quick-disconnect type of fuel-rod end fitting. The connector was devised in order to provide a means by which an irradiated multirod cluster could be remotely disassembled, the individual rods thoroughly examined, the cluster reassembled, and the element recharged into a reactor for additional irradiation. The test element was irradiated in KER-Loop 1 at HAPO. Fluid flow and heat transfer calculations and a description of the fabrication method and test conditions were reported (6, p. 1-21). Physics and reactor data were obtained and reported by Kratzer (45, p. 1-27). Ex-reactor flow tests were conducted and documented by Doman (24, p. 1-10). Irradiation conditions and cluster data are shown in Table XI.

Table XI - Results from IP 226A, Seven-Rod Cluster Irradiation Test

Rod No.	Length Change (in.) x 10 ⁻³ :		Increase in Single-Throw Warp, (in) x 10 ⁻³
	Core	Clad	
2		1	7
5	40	7	2
7		19	6
12		15	6
10		12	4
11		-1	8
9 (center)	47	20	8

General Information*

Exposure, Estimated	4.7 x 10 ²⁰ nvt
Coolant Conditions	1250-1300 psig, 230-310°C, pH 10
Fuel Material	Al-1.8 Pu alloy, extruded
Cladding, Tubes	Zircaloy-2, extruded
End Caps	Zircaloy-2, machined
Rod End Fixtures	Stainless steel (304 L Alloy) brackets and quick-disconnect, end cap fittings
Rod Size, OD	0.563 in.
Length	24 in.
Tube Wall	0.030 in.
Core OD	0.50 in.
Core Length	18.3 in., nominal
Assembly Method	Swage-size tubing onto cores (no lubricant used)
Tube ID-Core OD	0.003 - 0.004 in. (at 20°C)
Rod Spacing and Order	0.635 in., center-to-center; viewing pointed rod ends, rods in clock-wise order as listed above
Wire Wrapping, OD	0.072 in. (six outer rods wrapped)
Cluster Size, OD	2.08 in. (at ends)
Length	28 in.
Total Pu Content	20.31 gm

* See Appendix for estimate of precision of tabular values.

V. Fluid Flow, Heat Transfer, and Physics Calculations

Typical calculations for the alloy capsules irradiated in the MTR were based on the following conditions:

ID of MTR Stringer Basket	0.777 in.
OD of Capsule	0.568 in.
Length of Stringer Basket, l	3 ft.
Annulus Area, A_A	0.001522 sq. ft.
Jacket Thickness (Zircaloy-2, 3)	0.030 in.
OD of Alloy Fuel Core	0.050 in.
Specific Power, Q_1	30 kw/(ft of rod)
Power Generation, q'''	15.4 kw/(cu. in.)
Effective Pressure Drop to Induce Flow, Δp	35 psig
Effective Diameter, D_e	
Heat Transfer	0.0473 ft.
Hydraulic	0.0174 ft.
Coolant Properties,	
Temperature, t_w	115 F (46 C)
Density, ρ	61.8 lb/(cu ft)
Thermal Conductivity, k	0.37 Btu/(hr)(ft)(°F)
Dynamic Viscosity, μ	1.4 lb/(hr)(ft)
Prandtl Number, Pr	3.8

Mean Thermal Conductivity of Zircaloy, k_z (51, p. 302.1T)

$$8.4 \text{ Btu}/(\text{hr})(\text{ft})(^\circ\text{F})$$

Interface Thermal Conductance, h_i (75, p. 10)

$$5000 \text{ Btu}/(\text{hr})(\text{sq ft})(^\circ\text{F})$$

Assumptions which were made for the fluid flow computations are listed below:

- (a) MTR basket to be fully loaded with capsules.
- (b) Steady flow conditions to prevail in the uniform circular annulus.
- (c) Annulus to be completely filled with liquid.
- (d) Equilibrium conditions to be present.
- (e) Variation in liquid density small enough to neglect.

The fluid flow calculations were made as follows:

$$\Delta p = \frac{fG^2 l}{2Pg_c D_e} \quad (76, \text{HW-60996, p. 8-10})$$

$$G = 2540 \text{ lb}/(\text{sec})(\text{sq ft}) = 9.14 \times 10^6 \text{ lb}/(\text{hr})(\text{sq ft})$$

$$N_{RE} = De G/\mu = 1.136 \times 10^5 \text{ (turbulent flow)}$$

$$f = 0.018 \text{ (from Moody Diagram for smooth tube)} (66, \text{p. 130})$$

$$\text{Flow Velocity} = \frac{G}{\rho} = 41.1 \text{ ft}/\text{sec}$$

$$\text{Flow Rate} = GA_A = 27.9 \text{ gal}/\text{min.}$$

The heat transfer calculations were based on the following assumptions:

- (a) Coolant temperature uniform at any cross section of the stream.
- (b) Neglect gamma heating and fast flux contribution.

- (c) Neglect radiant-heat transfer and axial heat flow (13, p. 433).
- (d) Ignore end effects and other heat sources.
- (e) Uniform heat generation, q''' , in all cases, except those in which a self-shielding ratio must be applied.
- (f) All heat generated, Q , enters coolant stream.
- (g) Uniform heat generation and flux along length of capsule.
- (h) Use mean thermal conductivity values and assume values remain constant over temperature ranges encountered.
- (i) Steady state conditions present.

The heat transfer calculations were performed as follows:

- (a) Film Temperature Drop, Δt_f

Using the Modified Colburn Equation with a negative tolerance of 20 percent,

$$h_f = 0.8 b K ,$$

as recommended by the MTR (66, p. 39), it is found through trial and error methods, that the following equations yield the appropriate values for b , K , t_f , and Δt_f shown below:

$$\Delta t_f = \frac{Q_1 (3413)}{h_f \pi D} \quad (49, p. 187)$$

$$h_f = \frac{6.88 \times 10^5}{\Delta t_f} \text{ Btu/(hr)(sq ft)(}^\circ\text{F)}$$

$$K = \frac{V^{0.8}}{(12 D_e)^{0.2}} = 26.8 \quad (66, \text{ p. } 38)$$

$$b = 26.47 \left[\frac{k^{0.7} \rho^{0.8} c_p^{0.3}}{\mu^{0.5}} \right]_f = 372 \quad (66, \text{ p. } 37, 52)$$

Using the value $t_f = 158 \text{ F}$, where $t_f = t_w + \frac{\Delta t_f}{2}$,

the equations indicate that:

$$h_f = 7970 \text{ Btu}/(\text{hr})(\text{sq ft})(^\circ\text{F})$$

$$\Delta t_f = 86 \text{ F}$$

By comparison, the Dittus-Boelter equation (66, p. 37-38),

uses quantities evaluated at the bulk water temperature,

t_w , produces the following answers:

$$h_f = 0.023 \frac{k}{D_e} \left[\frac{D_e G}{\mu} \right]^{0.8} \left[\text{Pr} \right]^{0.4}$$

$$h_f = 7560 \text{ Btu}/(\text{hr})(\text{sq ft})(^\circ\text{F})$$

$$\Delta t_f = 91 \text{ F}$$

The Dittus-Boelter equation does not involve a trial-and-error solution and provides a more conservative value for the temperature difference in the capsule experiments. It was used to determine the actual in-reactor temperatures which are shown in a later section.

(b) Jacket Temperature Drop, Δt_j

$$\Delta t_j = \frac{Q_1 (3413)}{2\pi k_z} \ln \left(\frac{OD}{ID} \right) \quad (49, \text{ p. } 13)$$

$$\Delta t_j = 217 \text{ F}$$

(c) Interface Temperature Drop, Δt_i

Use the empirical value,

$$h_1 = 5000 \text{ Btu}/(\text{hr})(\text{sq ft})(^\circ\text{F}) \quad (75, \text{ p. } 10)$$

$$\Delta t_i = \frac{Q_1 (3413)}{h_1 \pi (ID)} \quad (49, \text{ p. } 187)$$

$$\Delta t_i = 154 \text{ F}$$

(d) Fuel Core Surface Temperature

$$t_s = t_w + \Delta t_f + \Delta t_j + \Delta t_i$$

$$t_s = 572 \text{ F}$$

(e) Fuel Core Temperature Drop, t_c

$$\Delta t_c = \frac{Q_1 (3413) (F_{SS})}{4\pi k} \quad (49, \text{ p. } 19)$$

where F_{SS} , the self-shielding factor, is equal to the ratio of the power generation with self-shielding to the power generation without self-shielding. The factor values are shown below and in Figure 4. The method of calculation is shown in a following section.

Note:
 ϕ_{cs} - neutron flux at core surface
 ϕ_{avg} - average neutron flux in transverse fuel core section

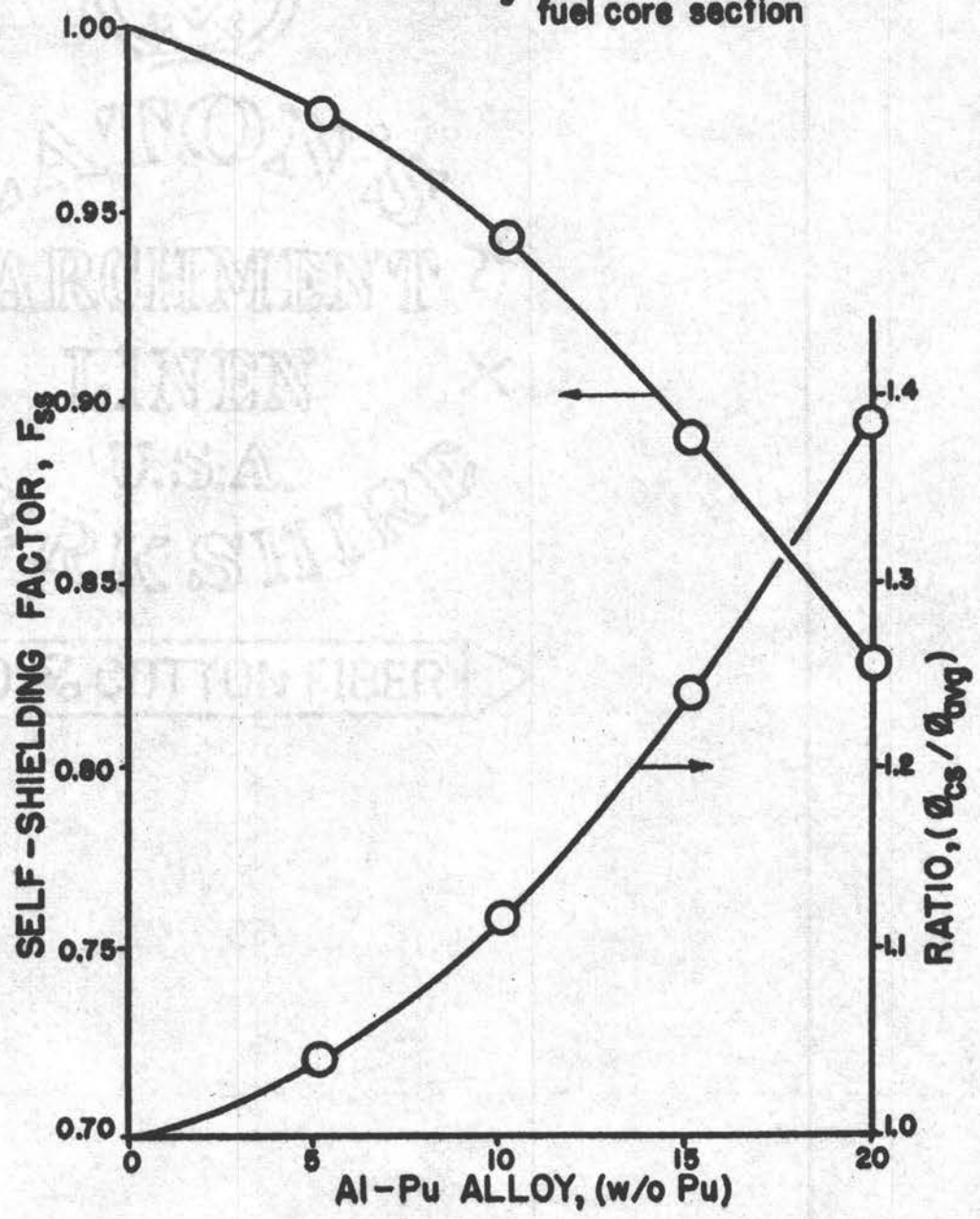


Fig. 4 - Self-Shielding Factor Values and Thermal Neutron Flux Ratios for Various Al-Pu Alloys.

Al-Pu or Al-12 Si-Pu Alloy (% Pu)	Self-Shielding Factor F_{ss}
1.65	> 0.99
1.80	> 0.99
5	0.975
8	0.960
10	0.943
15	0.889
20	0.828

To calculate the core temperature drop, it was first necessary to establish values for the mean thermal conductivities of the various alloys. A method for estimating the thermal conductivity of aluminum-plutonium alloys in the composition range 90-100 atomic percent aluminum has been reported (53, p. 5) (37, p. 2-9). The method was used and extended to the Al-12 Si-Pu alloys (70, p. 8). It was found that the thermal conductivity values for Al-12 Si-Pu alloys were about 0.7 of the values of aluminum-plutonium alloys with the same plutonium content. Briefly, the technique involved is to determine the ratio of free volume of aluminum (or aluminum-silicon) to the total volume and multiply the thermal conductivity of aluminum by this ratio to obtain the desired value. It is assumed that the plutonium is in the form of $PuAl_4$ and that the $PuAl_4$ has

essentially zero conductivity. Information on the exact form in which plutonium is present in the Al-12 Si-Pu alloys is not available as of this date. The density and thermal conductivity values used for the alloy capsule experiments were determined and the values are listed below:

Density Determinations

Al-Pu Alloy, (% Pu)	Calculated Density Values*		Measured Density Values	
	Using Al+Pu, gm/(cu cm)	Using Al+PuAl ₄ , gm/(cu cm)	Tensile Specimens** gm/(cu cm)	Capsule Cores, gm/(cu cm)
1.65	2.74	2.74	2.73	2.69 - 2.75
1.80	2.74	2.74	2.73	2.73 - 2.74
5	2.82	2.81	2.79	2.81
8	2.89	2.89	2.85	2.77 - 2.89
10	2.95	2.94	2.90	2.97 - 2.98
12.5	3.01	3.00	2.98	
15	3.09	3.07		2.98 - 3.00
20	3.24	3.22		3.19 - 3.26

* Densities used, gm/(cu cm): Al, 2.70; delta-phase Pu, 15.92; PuAl₄, 6.10.

** (34, p. 688-689)

Thermal Conductivity Values

<u>Al-Pu, Al-12 Si-Pu Alloy, (% Pu)</u>	<u>Volume of Free Al, %</u>	<u>$k_{\text{Al-Pu}}$ Btu/(hr)(ft)(°F)</u>	<u>$k_{\text{Al-Si-Pu}}$ Btu/(hr)(ft)(°F)</u>
1.65	98.9	132	93
1.80	98.8	131	92
5	96.6	128	90
8	94.5	126	88
10	93.0	124	87
15	89.0	118	83
20	84.6	113	79

Using the appropriate density, self-shielding factor, and thermal conductivity values, the following fuel core temperature drops were calculated:

<u>Fuel Core Temperature Drop, Δt_c, (°F)</u>		
<u>(% Pu)</u>	<u>Al-Pu Alloy</u>	<u>Al-12 Si-Pu Alloy</u>
1.65	61	87
1.80	62	88
5	62	88
8	62	89
10	62	88
15	61	87
20	60	85

(f) Maximum Fuel Core Temperature

$$t_{\max} = t_w + \Delta t_f + \Delta t_j + \Delta t_i + \Delta t_c$$

Maximum Fuel Core Temperature, t_{\max} , ($^{\circ}$ F)

<u>(% Pu)</u>	<u>Al-Pu Alloy</u>	<u>Al-12 Si-Pu Alloy</u>
1.65	634	659
1.80	635	660
5	635	660
8	635	661
10	635	660
15	634	659
20	633	657

(g) Maximum Heat Flux

$$H_F = \frac{(Q_1)(3413)(12)}{(OD)}$$

$$H_F = 689,000 \text{ Btu/(hr)(sq ft)}$$

Typical calculations for the $\text{UO}_2\text{-PuO}_2$ capsules are similar to those for the alloy capsules, with the following exceptions:

(a) High-density, $\text{UO}_2\text{-PuO}_2$ Capsules

(1) Conditions

Specific Power, $Q_1 = 19.2 \text{ kw/(ft of rod)}$

Power Generation, $q''' = 7.99 \text{ kw/(cu in.)}$

(2) Heat Transfer

Interface Temperature Drop

Use empirical value,

$$h_i = 2000 \text{ Btu/(hr)(sq ft)(}^\circ\text{F)} \quad (55, \text{ p. } 5)$$

$$\Delta t_i = 247 \text{ F}$$

(3) Maximum Fuel Core Temperature

For a first approximation of the core temperature, use the following equation (55, p. 2):

$$t_{\max} = (598 + t_s) \left(0.0599 Q_1 \frac{\rho_0}{\rho} \right)^{-598}$$

where ρ_0 is the theoretical density of the pellet and ρ is the actual density.

(4) Maximum Heat Flux

$$H_F = 440,000 \text{ Btu/(hr)(sq ft)}$$

(b) Low-Density, $\text{UO}_2\text{-PuO}_2$ Capsules

(1) Conditions

$$\text{Specific Power, } Q_1 = 12 \text{ kw/ft}$$

$$\text{Power Generation, } q''' = 4.99 \text{ kw/(cu in)}$$

(2) Interface Temperature Drop

Use empirical value,

$$h_i = 2,000 \text{ Btu/(hr)(sq ft)(}^\circ\text{F)} \quad (55, \text{ p. } 5)$$

$$\Delta t_i = 155 \text{ F}$$

(3) Maximum Fuel Core Temperature

For a cursory estimate of the core temperature use the following equation (55, p. 2):

$$t_{\max} = (598 + t_s) \cdot 0.0599 \frac{\rho_0}{\rho_{-598}}$$

$$t_{\max} = 2400 \text{ F}$$

(4) Maximum Heat Flux

$$H_F = 275,000 \text{ Btu/(hr)(sq ft)}$$

Typical physics calculations for the capsules irradiated in the MTR are shown below:

(a) Physics Calculations - Alloy Capsules

$$q''' = k_f \sum_f \phi, \text{ in watts/(cu cm)} \quad (76, \text{ HW-57343, p.8-9})$$

where:

(1) $k_f = 3.204 \times 10^{-11}$ (watt)(sec)/fission, if one assumes 200 mev/fission.

(2) $\sum_f = N \bar{\sigma}_f$ Pu, the macroscopic fission cross section (1/cm).

(3) N = nuclear density of fissionable plutonium, atoms/(cu cm). For calculation purposes, it was assumed that plutonium-240 content of the plutonium in the fuel elements was the same as that in the aluminum-plutonium alloy fuel elements fabricated and used in the Physical Constants Test Reactor (PCTR), which amounts to about six percent (9, p. 1-32)(36, p. 26).

$$N = \frac{(\% \text{ Pu})(6.023 \times 10^{23})(0.94)}{(100)(239)} (\rho_{\text{Alloy}})$$

(4) ρ_{Alloy} = alloy density, gm/(cu cm).

(5) σ_f^{Pu} = microscopic fission cross section, barns.

Since the MTR uses the 2200 m/sec convention in reporting the neutron flux values, the appropriate cross section value (including epithermal contribution) is:

$$\sigma_f^{\text{Pu}} = 959 \text{ barns}$$

(6) $\phi = f(r)$, the thermal neutron flux, a function of core radius, r ; neutrons/(sec)(sq cm).

Making the appropriate substitutions,

$$q''' = \frac{(3.204)(10^{-11})(\% \text{ Pu})(6.023)(0.94)(\rho_{\text{alloy}})(959)(\phi)}{(10^{-23})(100)(239)(10^{24})}$$

In order to solve this equation, one needs to determine the flux, ϕ , as a function of the core radius, r . Flux depression calculations were made by Peterson (76, HW-57343, p. 8-9) and are shown below. The relative thermal neutron flux, ϕ_i , at a given distance, r_i , from the core center or the ratio of the flux at r_i to the average flux, over the entire core cross-section, ϕ_{avg} , has been plotted as a function of r_i and is shown in Figure 5. For the Al - 1.8 w/o Pu alloy case, it was found that ϕ_i/ϕ_{avg} was 0.99 or greater. The ratio of the flux at the fuel rod surface to the average flux has been plotted and is shown in Figure 4 as a function of fuel rod composition.

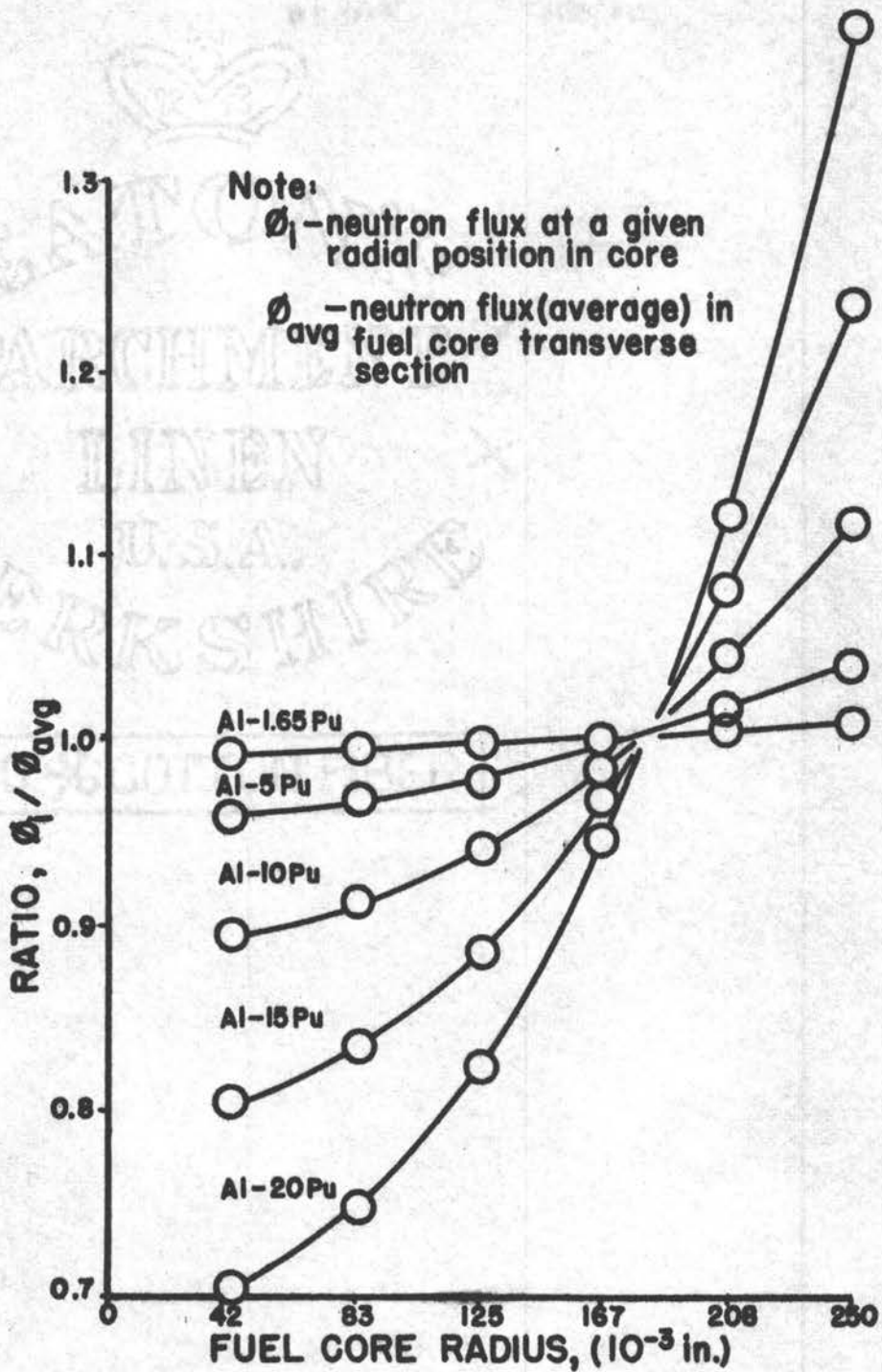


Fig. 5 - Ratio of Thermal Neutron Flux at a Given Radius to the Average Flux in the Transverse Section for Various Al-Pu Alloy Fuel Cores.

It was decided to fit equations of the form $y = a+bx+cx^2+dx^3+\dots$ to the curves shown in Figure 5 and thereby obtain ϕ as a function of r .

General equation:

$$\phi_1/\phi_{\text{avg}} = a+br_1+cr_1^2+dr_1^3+\dots, \quad (1)$$

where: ϕ_i = flux at r_i

ϕ_{avg} = Average flux over entire core

a, b, c, \dots = Constants

The first three terms in equation (1) were used and the higher power terms were neglected since they have relatively small effect. Flux-depression values were calculated using $r = r_i$ and $i = 1, 2, 3, 4, 5, 6$.

Flux Depression Data for Aluminum-Plutonium Alloys

<u>i</u>	<u>r_i, Distance from Core Center</u>		<u>Relative Flux at r_i or ϕ_i/ϕ_{avg} Al-Pu Alloy, (% Pu)</u>			
	<u>(cm)</u>	<u>(in.)</u>	<u>5</u>	<u>10</u>	<u>15</u>	<u>20</u>
1	0.106	0.042	0.962	0.894	0.802	0.704
2	0.212	0.083	0.969	0.912	0.833	0.747
3	0.317	0.125	0.979	0.942	0.887	0.823
4	0.423	0.167	0.995	0.985	0.969	0.944
5	0.529	0.208	1.016	1.044	1.083	1.123
6	0.635	0.250	1.041	1.118	1.239	1.386

Other Flux Ratios

ϕ_{avg} = average flux in fuel	1.000	1.000	1.000	1.000
$\phi_{moderator}/\phi_{avg}$	1.723	2.504	3.426	4.400
$\phi_{mod}/\phi_{core\ surface}, i=6$	1.655	2.240	2.765	3.177

For convenience, i-values of 1, 4, and 6, were used for determination of the constants a, b, and c in equation (1).

$$\phi_1/\phi_{avg} = a+b(0.106)+c(0.106)^2 \quad (2)$$

$$\phi_4/\phi_{avg} = a+b(0.423)+c(0.423)^2 \quad (3)$$

$$\phi_6/\phi_{avg} = a+b(0.635)+c(0.635)^2 \quad (4)$$

Solving the three equations simultaneously, one obtains the following expressions for a, b, and c:

$$b = 3.155 \left(\frac{\phi_4}{\phi_{avg}} - \frac{\phi_1}{\phi_{avg}} \right) - 0.5290 c \quad (5)$$

$$c = 8.889 \left(\frac{\phi_6}{\phi_{avg}} \right) - 14.81 \left(\frac{\phi_4}{\phi_{avg}} \right) + 5.926 \left(\frac{\phi_1}{\phi_{avg}} \right) \quad (6)$$

$$a = \left(\frac{\phi_1}{\phi_{avg}} \right) - 0.106 b - 0.01124 c \quad (7)$$

Now $q''' = k_f \sum_f \phi$, in watts/(cu cm), and

$$\phi = \phi_{avg} [a + br + cr^2]$$

Let $Q_1 = kw$ /(ft of rod length),

$v =$ Volume of core material in (cu cm)(ft of rod),

and $d_v = (12)(2.54)(2\pi r)dr$.

Then $dQ_1 = (10^{-3})(q''')(2\pi)(r)(12)(2.54)dr$, or

$$dQ_1 = (10^{-3})(k_f)(\sum_f)(\phi_{avg})(a+br+r^2)(2\pi r)(12)(2.54)dr.$$

Let $X = (10^{-3})(k_f)(\sum_f)(\phi_{avg})(2\pi)(12)(2.54)$ and make the substitution to get

$$dQ_1 = X \int_0^r (ar+br^2+cr^3) dr$$

$$Q_1 = X \left[\frac{ar^2}{2} + \frac{br^3}{3} + \frac{cr^4}{4} \right] kw/(ft of rod) \quad (8)$$

To obtain Δt_c , where $\Delta t_c = t_{max.} - t_s$, $t_s =$ core surface temperature, and $t_{max.} =$ core center temperature (maximum), substitute Q_1 from equation (8) into the following expression:

$$(3413)Q_1 = -(2\pi r) k \frac{dt}{dr} \quad (49, p. 19)$$

$$(3413)(X) \left(\frac{ar^2}{2} + \frac{br^3}{3} + \frac{cr^4}{4} \right) = -2\pi kr \frac{dt}{dr}$$

$$(3413)(X) \int_0^r \left(\frac{ar}{2} + \frac{br^2}{3} + \frac{cr^3}{4} \right) dr = -2\pi k \int_{t_{\max}}^{t_s} dt$$

$$(3413)(X) \left[\frac{ar^2}{4} + \frac{br^3}{9} + \frac{cr^4}{16} \right]_0^r = -2\pi k(t_s - t_{\max.})$$

$$\Delta t_c = \frac{3413 X}{2\pi k} \left[\frac{ar^2}{4} + \frac{br^3}{9} + \frac{cr^4}{16} \right] \quad (9)$$

$$\Delta t_c = \frac{3413 Q_1}{2\pi k} \frac{\left[\frac{ar^0}{4} + \frac{br^1}{9} + \frac{cr^2}{16} \right]}{\left[\frac{ar^0}{2} + \frac{br^1}{3} + \frac{cr^2}{4} \right]} \quad (10)$$

Now to aid in detecting the difference between the uniform-heat-generation case, $\Delta t_c = \frac{3413 Q_1}{4\pi k}$, and equation (10), arrange (10) as follows:

$$\Delta t_c = \frac{3413 Q_1}{4\pi k} \frac{\left[\frac{a}{4} + \frac{br}{9} + \frac{cr^2}{16} \right]}{\left[\frac{a}{4} + \frac{br}{6} + \frac{cr}{8} \right]} \quad (11)$$

Now using equations (5), (6), and (7) and the values for $\phi_1 / \phi_{\text{avg}}$ one can solve equation (11) for Δt_c for a given alloy case as shown below. The self-shielding factor, F_{SS} , is the value obtained from the bracketed quantity in equation (11). Values for F_{SS} for the various alloys are shown in the section on heat transfer calculations and in Figure 7. Values for the constants in equation (11) for the aluminum-plutonium alloy cases were calculated for $r = 0.635$ cm and are listed below. It was assumed that the values could be used for the Al-Si-Pu

alloy cases with the same plutonium concentration.

Al-Pu Alloy, % Pu	Constants in Equation Eleven			
	a	b	c	F _{SS}
1.65	--	--	--	> 0.99
1.8	--	--	--	> 0.99
5	0.9608	-0.0112	0.218	0.975
10	0.8926	-0.0557	0.648	0.943
15	0.8096	-0.2216	1.415	0.889
20	0.7363	-0.5711	2.511	0.828

Using equation (8), $r = 0.635$ cm, and the appropriate values for a, b, and c, one can calculate Q_1 for a given alloy case.

$$Q_1 = X \left[\frac{ar^2}{2} + \frac{br^3}{3} + \frac{cr^4}{4} \right]$$

$$Q_1 = (10^{-3})(k_f)(\Sigma_f)(\phi_{avg})(2\pi)(12)(2.54) \left[\frac{ar^2}{2} + \frac{br^3}{3} + \frac{cr^4}{4} \right]$$

Values for $\phi_{\text{core surface}} = \phi_{\text{CS}}$ were computed for fixed values of Q_1 and are shown below:

Thermal Neutron Flux as a
Function of Specific Power Generation

Al-Pu and Al-12 Si-Pu Alloys, (% Pu)	$\phi_{\text{Core Surface, (nv x 10}^{13}\text{)}}$					
	$Q_1 \text{ kw/(ft of rod)}$					
	25	30	35	40	45	50
1.65	20	24	27	31	35	39
1.80	18	22	25	29	32	36
5	6.1	7.3	8.6	9.8	11	12
10	2.7	3.2	3.7	4.3	4.8	5.3
15	1.6	1.9	2.2	2.5	2.8	3.1
20	1.0	1.2	1.4	1.6	1.8	2.0

From the flux depression data listed earlier, the following values for thermal neutron flux were computed.

Thermal Neutron Flux Ratios

Al-Pu Alloy, (% Pu)	$\frac{\phi_{\text{average}}}{\phi_{\text{core surface}}}$	$\frac{\phi_{\text{moderator}}}{\phi_{\text{core surface}}}$
1.65, 1.8	> 0.99	--
5	0.960	1.66
10	0.895	2.24
15	0.808	2.77
20	0.722	3.18

The fractional burnup (F.B.) of the atoms of a given fissionable isotope may be estimated by using the following equation:

F.B. = fraction of original fissionable atoms fissioned

$$F.B. = \left(1 - e^{-\bar{\sigma}_a \phi t} \right) \left(\frac{\bar{\sigma}_f}{\bar{\sigma}_a} \right) \quad (40, \text{ vol. 1, p. 63})$$

where:

	<u>Pu-239</u>	<u>U-235</u>
$\bar{\sigma}_a =$	1424 barns	664 barns
$\bar{\sigma}_f =$	959 barns	554 barns
$\phi =$	thermal neutron flux, neutrons/(sec)(sq cm)	
$t =$	time, sec	
$t =$	exposure, nvt = neutrons/(sq cm)	

(Note - microscopic cross section values include the epithermal contribution)

(b) Physics Calculations - UO₂-PuO₂ Capsules

The values for the macroscopic fission cross sections and flux ratios for the UO₂-PuO₂ capsules were determined by Peterson and Regimbal (76, HW-59365, p. 7). The data for high and low density UO₂-PuO₂ capsules are shown below.

It was decided to irradiate all oxide specimens for two MTR cycles or to an exposure of about 1000 megawatt-days per ton. It was planned to inspect all capsules after discharge, metallographically examine one of each capsule pair, and recharge the remaining capsules for irradiation to higher exposure, on the order of 5000 megawatt-days per ton.

UO₂-PuO₂ (Density - 90 Percent of Theoretical Value)

UO ₂ -PuO ₂ (a/o PuO ₂)	Thermal Neutron Flux Ratios*		Macroscopic Fission Cross Section, Σ_f ; (cm ⁻¹)
	ϕ_{avg}/ϕ_{cs}	ϕ_{cc}/ϕ_{cs}	
0.0259	0.974	0.95	0.0811
1.02	0.926	0.86	0.254
2.57	0.840	0.70	0.525
4.13	0.753	0.56	0.796
5.67	0.674	0.44	1.066

UO₂-PuO₂ (Density - 70 Percent of Theoretical Value)

0.0259	0.980	0.97	0.0836
0.187	0.978	0.96	0.0848
1.46	0.927	0.88	0.258
3.47	0.848	0.72	0.528
5.46	0.762	0.57	0.798
7.45	0.682	0.45	1.07

* ϕ_{avg} = average flux in fuel core cross-section,

ϕ_{cs} = flux at core surface, and

ϕ_{cc} = flux at core center (extrapolated value).

VI. Fabrication of Test Specimens

In general, the alloy capsules were fabricated in the following manner. Elemental plutonium was melted along with aluminum or aluminum-silicon alloy (eutectic composition) to form a master alloy with approximately 15 percent plutonium. The cast master alloy was remelted and the appropriate material added to obtain the desired final alloy composition. The alloy melt was cast into molds made from reactor-grade graphite. The melting and casting operations were performed in both vacuum and air-atmosphere furnace units. The melt, pour, and mold temperatures and the particular method employed for the preparation of the fuel alloys are shown below:

Al-Pu Alloy, (% Pu)	Approximate Temperatures, (°C)			Furnace Atmosphere	
	Melt	Pour	Mold	Master Alloy	Final Alloy
1.65	850	700	240-280	Vacuum	Vacuum
1.80	800	700	100	Air	Air
5	800	700	100	Air	Air
8	825	700	100	Air	Air
10	825	700	100	Air	Air
15	925	730	100	Air	Air
20	950	775	100	Air	Air

The alloy cores for the first and second capsule sets were produced by Koler (76, HW-51854, p. 11) (76, HW-51855, p. 2-7). All other alloy cores for capsule and cluster tests were cast by Bloomster (76, HW-57433, p. 7).

The cast alloy rods, about 5/8-inch in diameter and 6 to 12 inches in length, were radiographed and sampled for chemical analysis, spectrographic analysis, and metallographic examination. The fuel cores for the capsules were machined from the cast rods. The machined fuel cores were normally on the order of 1/2-inch in diameter by 2.0 inches long. The alloy cores were stamped on one end with an identity number. With the exception of the first two capsule sets, all alloy cores were used in the annealed condition. The alloy cores were annealed by holding them at 400 - 450 C for one hour in an air atmosphere. To prepare the cores for loading into Zircaloy cladding components, the fuel pieces were degreased, weighed, measured, and photographed.

The jacketing components for the alloy capsules were fabricated by several methods. For the first and second capsule experiments, the Zircaloy-2 cladding parts were machined from solid bar stock. In all of the other alloy capsule sets, the end caps were machined from Zircaloy-2 bar stock and the tube sections were cut from seamless, extruded Zircaloy-3 tubing. The Zircaloy used for the capsules was nondestructively

examined by radiography, hydrostatic testing, eddy-current testing, and penetrant testing. The materials were sampled for metallographic examination, chemical analysis, spectrographic analysis, and corrosion testing.

The Zircaloy tube section was joined to an end cap by fusion welding. The components were degreased in trichloroethylene and areas on the parts in the vicinity of the weld zone were etched in HNO_3 - HF prior to the welding operation. The assembly or can was tested for leaks by means of a helium leak detector. The can interiors were measured by micrometer and prepared to receive the fuel alloy cores. An attempt was made to match fuel cores to cans so that under reactor operating conditions the fuel cores would just come in intimate contact with the cylindrical can surface. With such a fit, a good heat transfer path would result and the effect of the marked difference in the coefficient of thermal expansion between the core and cladding would be reduced. In order to prevent radioactive weld zones, the can opening was counter-bored and fitted with a brass bushing. The bushing was taped to the can OD and the can inserted into and taped to a specially designed plastic bag which sealed to a standard glove port in a plutonium-handling facility. The can was attached to the plastic bag in such a manner that only the interior surface was exposed to the radioactive contamination as shown in

Figure 3. The fuel core was slipped into the can and a narrow band of the plastic bag near the can opening was fused together with an electronic sealer. The capsule assembly was released from the main portion of the bag by cutting through the fused area. The capsule assembly was placed in an evacuable welding chamber along with a filter plug and the other end cap. Inside of the sealed welding chamber, the residual plastic bag and the brass protector were carefully removed and canned for disposal. The filter plug, a polyethylene piece with a hole packed with pyrex wool, was firmly seated in the open can end. The welding chamber was sealed, evacuated to a pressure of 25 - 50 microns or less of mercury, and filled with helium until atmospheric pressure was attained. The filter plug was removed and the etched end cap placed in the can opening. The final closure was made by fusion welding. All welding on Zircaloy cladding components for capsule and cluster tests was done by Lemon (46, p. 13) (76, HW-51854, p. 6, 7, 12, 14) (76, HW-57342, p. 18, 21) and all welds were made in a helium atmosphere. The welds were effected without filler metal and were produced by using the direct-current, tungsten-inert-gas process.

The welded capsule was removed from the chamber, surveyed for possible contamination, weighed, and stamped on one end with the irradiation test identification. The capsule was

tested with the helium leak detector and/or with a "bubble" tester. The capsule was etched in HNO_3 -HF and autoclaved for 100 hours at 170 C and 100 pounds per square inch (gage). The capsule was supported by a stainless steel basket and deionized or distilled water was used to partially fill the autoclave. The autoclaved capsule was visually inspected, weighed, measured, radiographed, and photographed. The irradiation test identification number was stenciled on the cylindrical surface of the autoclaved capsule by grit blasting with alumina. The stenciling removes less than 0.005 inch of material yet provides a large, recognizable number which is an item of major importance when the irradiated specimen is discharged.

In the case of the UO_2 - PuO_2 capsules all pellets were about 1/2-inch in diameter and 0.6 - 0.7 inch in length and the fabrication method differed from that of the alloy capsules in the following ways:

(a) Fifth Capsule Experiment (GEH-14-19 and 20)

UO_2 - PuO_2 mixed-crystal-oxide (UO_2 : PuO_2 ::5:1) was added to natural UO_2 (PWR grade) to bring the concentration of PuO_2 down to 0.0259 atomic percent. The material was ball milled, cold pressed, and then sintered at 1600 C for one hour. The high-density compacts, about 90 percent of the theoretical value, were ground to final dimensions and

placed in fully-machined, Zircaloy-2 cladding. There were two pellets per capsule and the pellets were 0.001-inch smaller in diameter than the tubing ID.

(b) Sixth Capsule Experiment (GEH-14-21 and 22)

PWR-grade, natural UO_2 was added to UO_2 - PuO_2 , mixed-crystal-oxide ($UO_2:PuO_2::5:1$) to lower the PuO_2 concentration to 0.0259 atomic percent. The UO_2 had been ball milled for 48 hours. Carbowax 20M was used as a binding agent. The material was cold pressed to a density of about 65 percent of the theoretical value. The pressed compacts were placed in a furnace and heated in a hydrogen atmosphere to 1000 C in order to volatilize the binding agent. There was no soak time at the elevated temperature and the pieces were allowed to cool in the hydrogen atmosphere. The pellets were loaded into fully-machined, Zircaloy-2 cladding components. The cladding ID was 0.002 inch larger than the pellet diameter. There were three pellets per capsule.

(c) Seventh Capsule Experiment (GEH-14-82 through 91)

The fuel material consisted of a mechanical mixture of PuO_2 and UO_2 . The PWR-grade, natural UO_2 was ball milled for 48 hours. The binding agent was Carbowax 20M. The material was cold pressed (50,000 psi) to approximately 65 percent of theoretical density. The green

pellets were sintered and cooled in a hydrogen atmosphere.

The heating rate was approximately 100 C per hour.

Sintering conditions for the capsule pellets were as

follows:

UO_2 - PuO_2 (a/o PuO_2)	GEH-14 Number	Temperature (°C)	Time at Temperature, (hr)
0.0259	90, 91	1500	11
1.02	82, 83	1600	4
2.57	84, 85	1600	4
4.13	86, 87	1600	No soak time
5.67	88, 89	1600	No soak time

The sintered compacts were ground to final dimensions.

The pellets were 0.002 inch smaller in diameter than the cladding ID. Three compacts were placed in each capsule.

Fully machined Zircaloy-2 components were used.

(d) Eighth Capsule Experiment (GEH-14-65 through 74)

PuO_2 was added to PWR-grade, natural UO_2 to form mechanical mixtures in which the concentration of PuO_2 was 0.187, 1.46, 3.47, 5.46, and 7.45 atomic percent.

The UO_2 had been ball milled for 48 hours. Carbowax 20M was the binding agent used. The material was cold pressed to a density of about 65 percent of the theoretical value.

The pressed pellets were placed in a furnace and heated in a hydrogen atmosphere to 1000 C to drive off the binding agent. There was no soak time at the elevated

temperature and the specimens were allowed to cool in the hydrogen atmosphere. The ID of the fully-machined, Zircaloy-2 cladding was 0.002 inch larger in diameter than the pellet OD.

For the ninth experiment, the four-rod cluster element (IP 186A) with alloy fuel cores, the fabrication method was similar to the one used for the alloy capsules with the following exceptions. The cluster was about ten inches long, had an active fuel core length of eight inches, and had center-to-center spacing on the fuel rods of 0.75 inch. The cast fuel cores were Al-8 Pu and Al-12 Si-8 alloy and were four to eight inches in length. Zircaloy-3 tubing and Zircaloy-2 end caps were used for fuel rod cladding. The welded fuel rods were autoclaved in steam at 300 C and 1275 pounds per square inch (gage) for 72 hours. The autoclaved rods were not stenciled and were assembled into a cluster by means of stainless steel clips and bands. The bands were slightly compressed in order to charge the element in the reactor process tube. Once in the tube, the bands on the fuel cluster expanded and held the element in position. The clip-band fixtures were used in an effort to reduce the tendency of the light element to vibrate and chatter during irradiation. The stainless steel parts were joined by Heliarc spot welding. No stainless steel parts were welded to the Zircaloy cladding. A cluster for flow tests

in an ex-reactor loop facility, was fabricated with aluminum cores and stainless steel cladding. The tests were performed by Doman and have been reported (24, p. 1-2).

In the tenth experiment, IP 226A, a seven-rod cluster element was irradiated. The fabrication of this element differed from the alloy capsule fabrication method in the following respects. Cast billets of Al-1.8 Pu alloy were hot extruded into 1/2-inch diameter rods from which were cut the fuel cores for the cluster test. The extrusion data are shown below:

Al-1.8 Pu Alloy Extrusion Conditions

Extrusion Billet and Container Temperature	500 C
Extrusion Die Temperature	350 C
Extrusion (Ram) Speed	20 in./min
Reduction in Area	98 percent
Extrusion Constant	24,600 psi

The extruded rods were straightened and machined to length (18.5 inches). All extrusion and straightening operations were performed and reported by Ross

(76, HW-61994, p. 28-31). The fuel rods were clad with extruded Zircaloy-2 tubing and Zircaloy-2 end caps. After welding, the clad fuel rods were swaged to obtain a difference of 0.003 - 0.004 inch between the core OD and the cladding ID. The wire-wrapped swaged rods were autoclaved in steam at 400 C and 1500 pounds per square inch (gage) for 72 hours) The

autoclaved rods were assembled into cluster form with quick-disconnect fittings and stainless steel end fixtures. The fittings and fixtures were designed and prepared by Sharp (76, April-June, 1960). The fuel rod preparation and cluster assembly were directed by Freshley (76, April-June, 1960). A similar cluster with stainless steel cladding and aluminum cores was fabricated for flow tests. The tests were conducted and reported by Doman (24, p. 3-10). All clusters were 28 inches in length, about 2.08 inches in diameter, and had single-piece cores, 18.5 inches in length. The clusters duplicate as nearly as possible the appearance and construction of the center rod and six-rod ring of one of the candidate designs for the PRTR fuel elements.

VII. Zircaloy Tubing Problem

Extruded and tube-reduced, Zircaloy-2 tubing of the Mark-I, PRTR-type (0.505-inch ID by 0.030-inch wall thickness) was used for cladding on capsules and prototypical cluster elements for irradiation tests and for exploratory ex-reactor work, such as thermal cycling of simulated fuel rods, injection casting of full-length PRTR fuel rods, and fabrication of flow-test and corrosion samples. Inspection of the as-received tubing and examination of fabricated specimens indicated that the tubes contained longitudinal cracks or defects. The defects were predominantly on the inner surface of the tubes. The presence

of similar defects on the interior surfaces of Zircaloy-2 tubing has been reported by other investigators (25, p. 1-16).

The tubes were evaluated by subjecting samples to the following examinations:

- (a) Fluorescent penetrant test of inner and outer tube surfaces (both on short, four-inch sections, and on full-length 90 inch tubes),
- (b) Eddy current test of OD and ID of tubes,
- (c) Corrosion test in high pressure and temperature water,
- (d) Measurement of surface finish (OD and ID, both parallel and perpendicular to extrusion direction),
- (e) Metallographic inspection (including wall thickness measurements, hardness, and determination of size, type, relative number, and location of defects, and grain size),
- (f) Dimensional inspection (including air gaging of OD and ID and wall thickness measurements),
- (g) Flare and flattening tests,
- (h) Chemical and spectrographic analyses,
- (i) Ultrasonic flaw test, and
- (j) Tensile Test.

VIII. Evaluation Techniques

It was planned to judge the performance of the irradiated capsule and cluster specimens by evaluating results from the following:

- (a) Actual in-reactor conditions and capsule or cluster operation,
- (b) Visual examination of the discharged specimen,
- (c) Ease of disassembly,
- (d) Dimensional measurements on the clad samples and in the case of the alloy capsules, the dejacketed cores,
- (e) Density determination (alloy cores only),
- (f) Burnup analysis,
- (g) Fission gas release and analysis (oxide capsules only),
and
- (h) Metallographic examination, including hardness, photomacrographs, photomicrographs, and replicas.

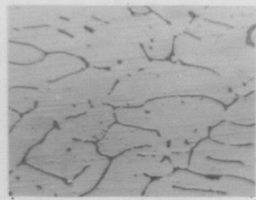
RESULTS AND CONCLUSIONS

All of the capsule and cluster fuel element specimens employed in the ten experiments described herein performed satisfactorily during irradiation. One irradiated, high-density, UO_2 - PuO_2 capsule (GEH-14-89) ruptured when it was reinserted into the reactor and inadvertently placed in a neutron flux eleven times higher than the specified value. Data on the actual irradiation test conditions for all ten experiments are shown in Tables II-XI. Photographs and graphical and tabular information pertaining to the irradiated specimens and to the tests conducted on Zircaloy tubing may be seen in Figures 6-18 and Tables XII and XIII. Burnup analyses were obtained on a number of specimens and confirmed the calculated values within the possible experimental error.

All specimens were visually examined at time of discharge and, except for the ruptured piece, were in very good condition. No hot-spot indications were noted and no excessive or unusual corrosion was observed, except on GEH-14-89. Visual inspection of all samples at the Radiometallurgical Laboratory was performed. The inspection verified the results of the earlier cursory examination at the reactor basin. The radiometallurgical examination of the specimens was conducted by Brandt (Experiments 1 and 4), Gruber (Experiments 3, 4, 8, and 9), McMahan (Experiments 5 and 7), Teats (Experiments 2 and 10, and Zimmerman (Experiments 1 and 2).

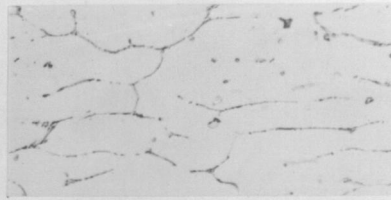
Typical irradiated alloy elements are shown in Figures 6-9, 13 and 14. Metallographic examination has been performed to data on 25

IRRADIATED AL-Pu ALLOYS



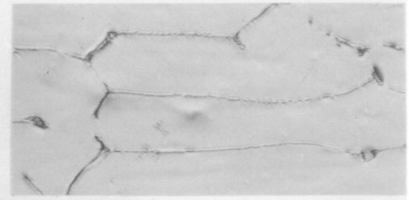
(0)

Al-1.65w/oPu



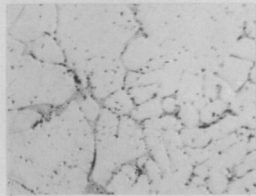
3-24-9

(47)



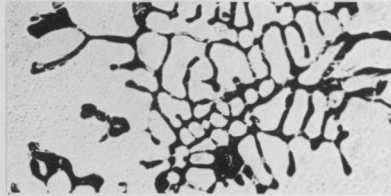
14-23

(61)



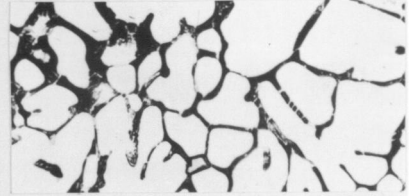
(0)

Al-5w/oPu



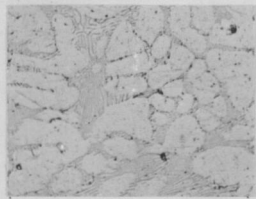
14-8

(80)



14-45

(80)



(0)

Al-10w/oPu



14-5

(45)



14-43

(89)



(0)

Al-15w/oPu



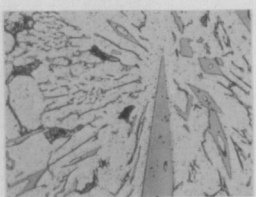
14-9

(75)



14-44

(105)



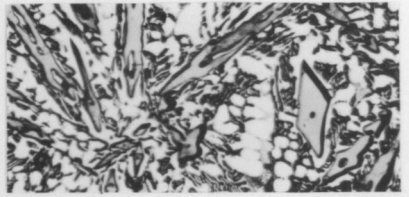
(0)

Al-20w/oPu



14-10

(47)



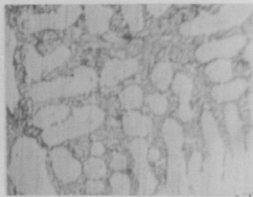
14-42

(77)

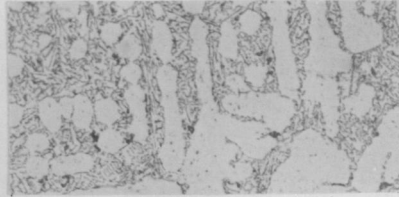
NOTE: X-Y=GEH CAPSULE NO., (Z)= 10^{18} FISSIONS/CM,
ALL (250X).

Fig. 6 - Pre-and Post-Irradiation Photomicrographs of Al-Pu Alloys.

IRRADIATED AL-SI-PU ALLOYS

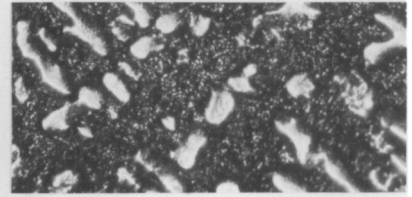


(0)



3-24-8

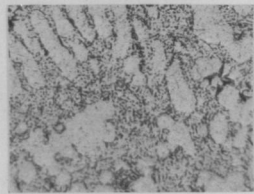
(50)



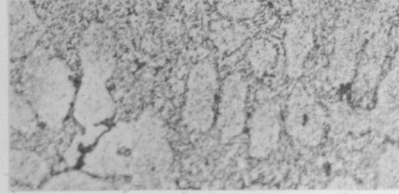
14-26

(65)

Al-12w/oSi-1.65w/oPu



(0)



14-6

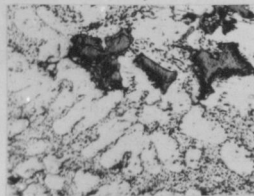
(39)



14-48

(79)

Al-12w/oSi-5w/oPu

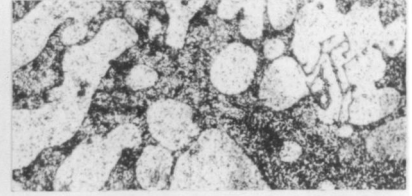


(0)



14-11

(35)



14-47

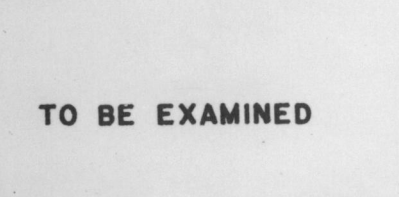
(94)

Al-12w/oSi-10w/oPu



(0)

TO BE EXAMINED



14-46

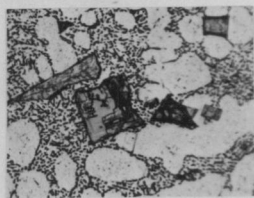
(56)



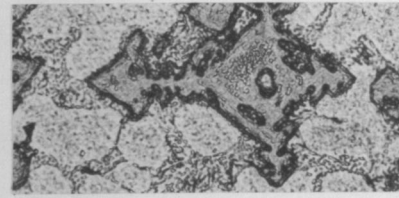
14-7

(69)

Al-12w/oSi-15w/oPu



(0)



14-12

(39)



14-49

(83)

Al-12w/oSi-20w/oPu

NOTE: X-Y= GEH CAPSULE NO., (Z)= 10^{18} FISSIONS/CU CM,
ALL (250X).

Fig. 7 - Pre-and Post-Irradiation Photomicrographs of Al-Si-Pu Alloys.

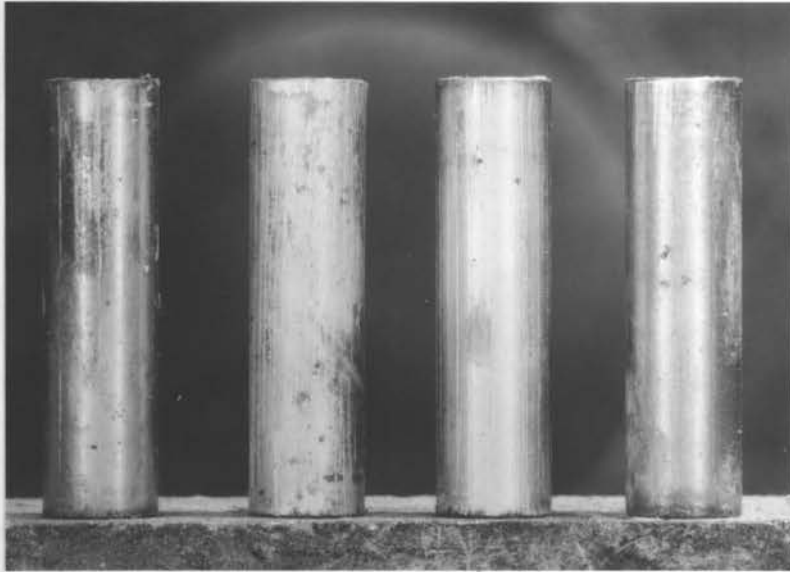
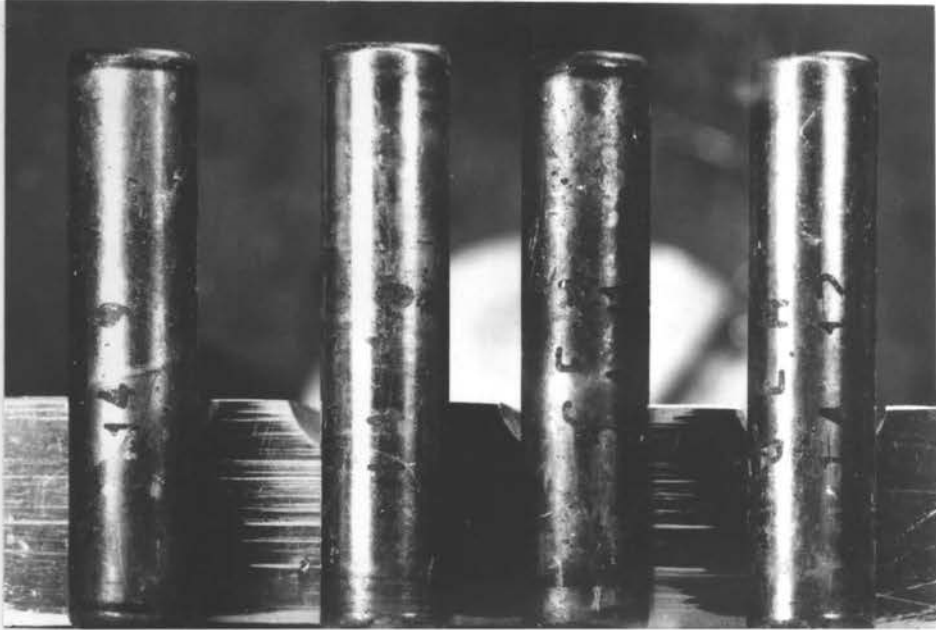
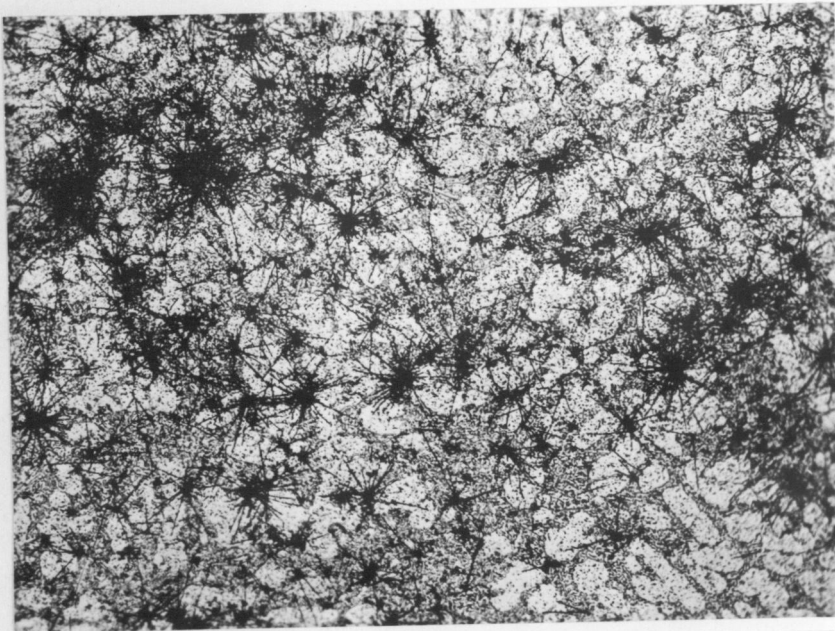


Fig. 8 - View of Irradiated Capsules and De-jacketed Alloy Fuel Cores.



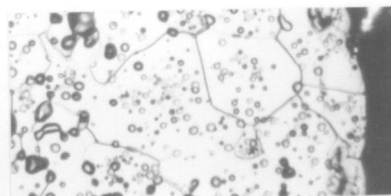
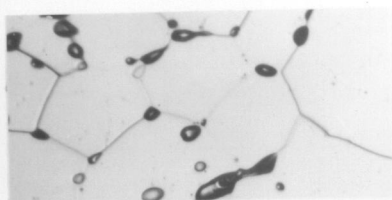
Al-1.65 w/o Pu Alloy (Capsule 3-24-9)



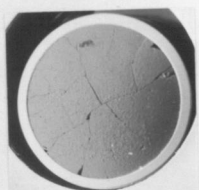
Al-12 w/o Si-1.65 w/o Pu Alloy (Capsule 3-24-8)

Fig. 9 - Photomicrographs of Irradiated Al-Pu and Al-Si-Pu Alloy Fuel Cores. Autoradiographic Technique Used to Show Location of Plutonium. (250X)

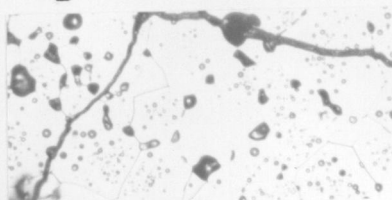
CORES 0.5 in. DIAM.

14-19, 0.0259 a/o PuO₂ CENTER

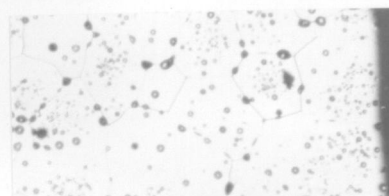
EDGE



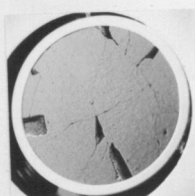
14-90, 0.0259



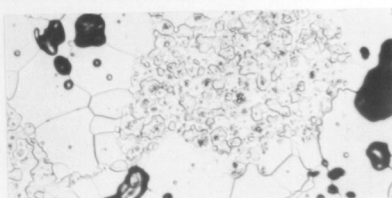
CENTER



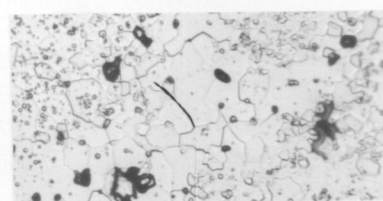
EDGE



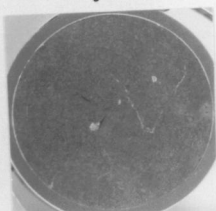
14-83, 1.02



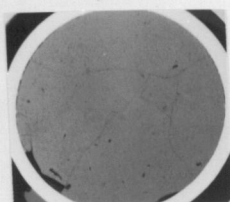
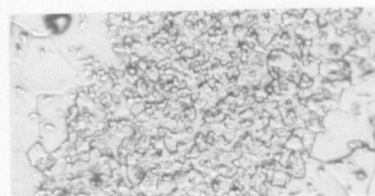
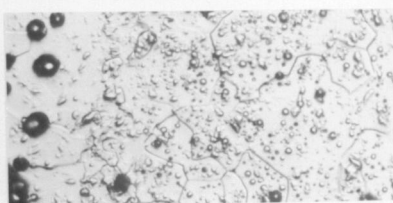
CENTER



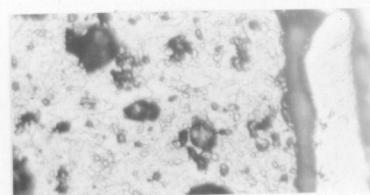
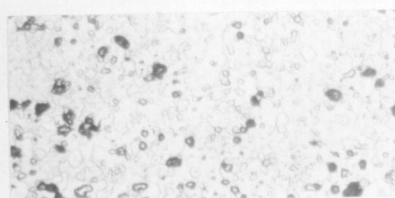
EDGE



14-84, 2.57

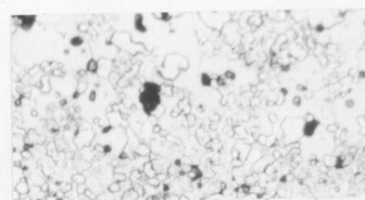
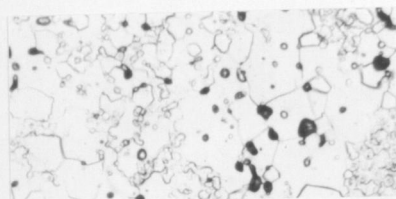


14-87, 4.13



UNIRRAD.

14-88, 5.67



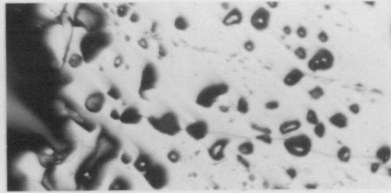
ALL(250X)

Fig. 10 - Irradiated, High-Density UO₂-PuO₂ Capsules.

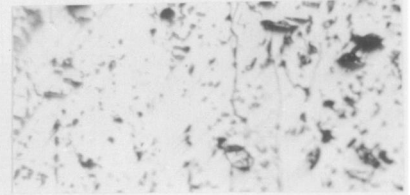
CORES 0.5in. DIAM.



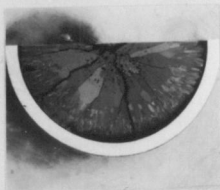
14-21, 0.0259 a/o PuO



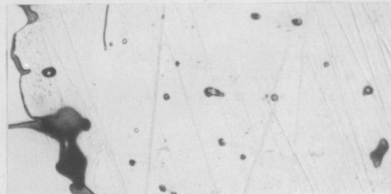
(100X)



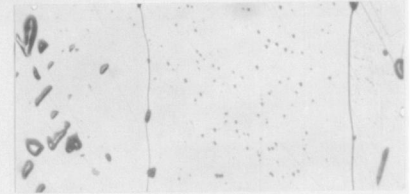
(100X)



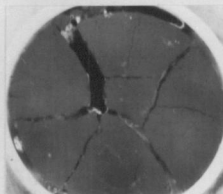
14-65, 0.187



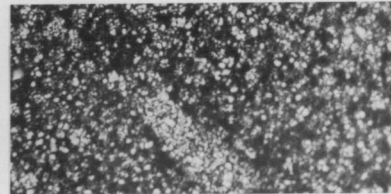
CENTER



EDGE



14-67, 1.46



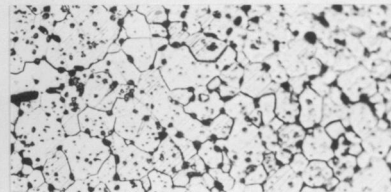
CENTER



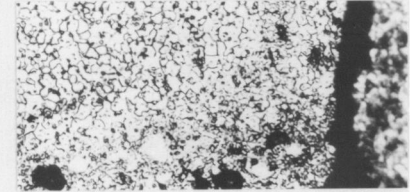
EDGE (500X)



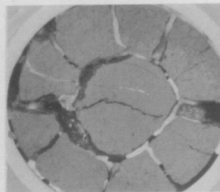
14-70, 3.47



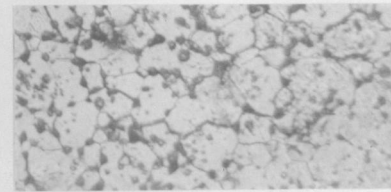
CENTER



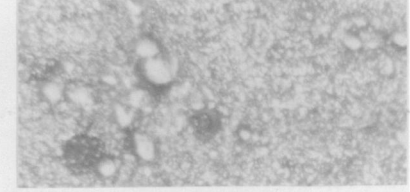
EDGE



14-72, 5.46



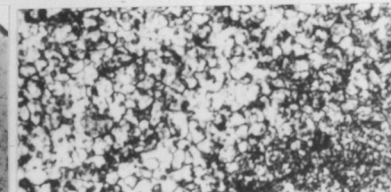
CENTER



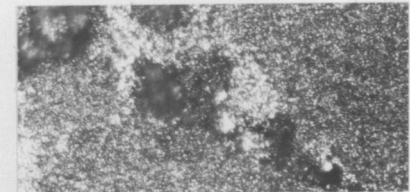
EDGE

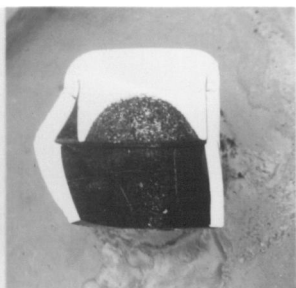


14-74, 7.45

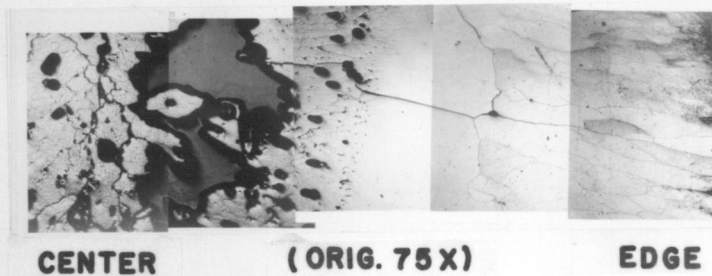


(250X) UNLESS MARKED

Fig. 11 - Irradiated, Low-Density UO_2 - PuO_2 Capsules.



GEH-14-89
 Desired Flux 0.2×10^{14} nv
 Actual Flux $\sim 2.2 \times 10^{14}$ nv



GEH-14-65

GEH-14-21

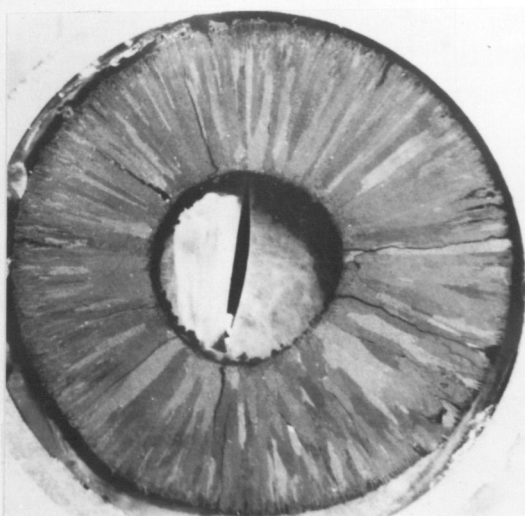


Fig. 12 - Appearance of Ruptured, High Density UO_2 - PuO_2 Capsule and of Central Void Formations in Low-Density, UO_2 - PuO_2 Capsules.

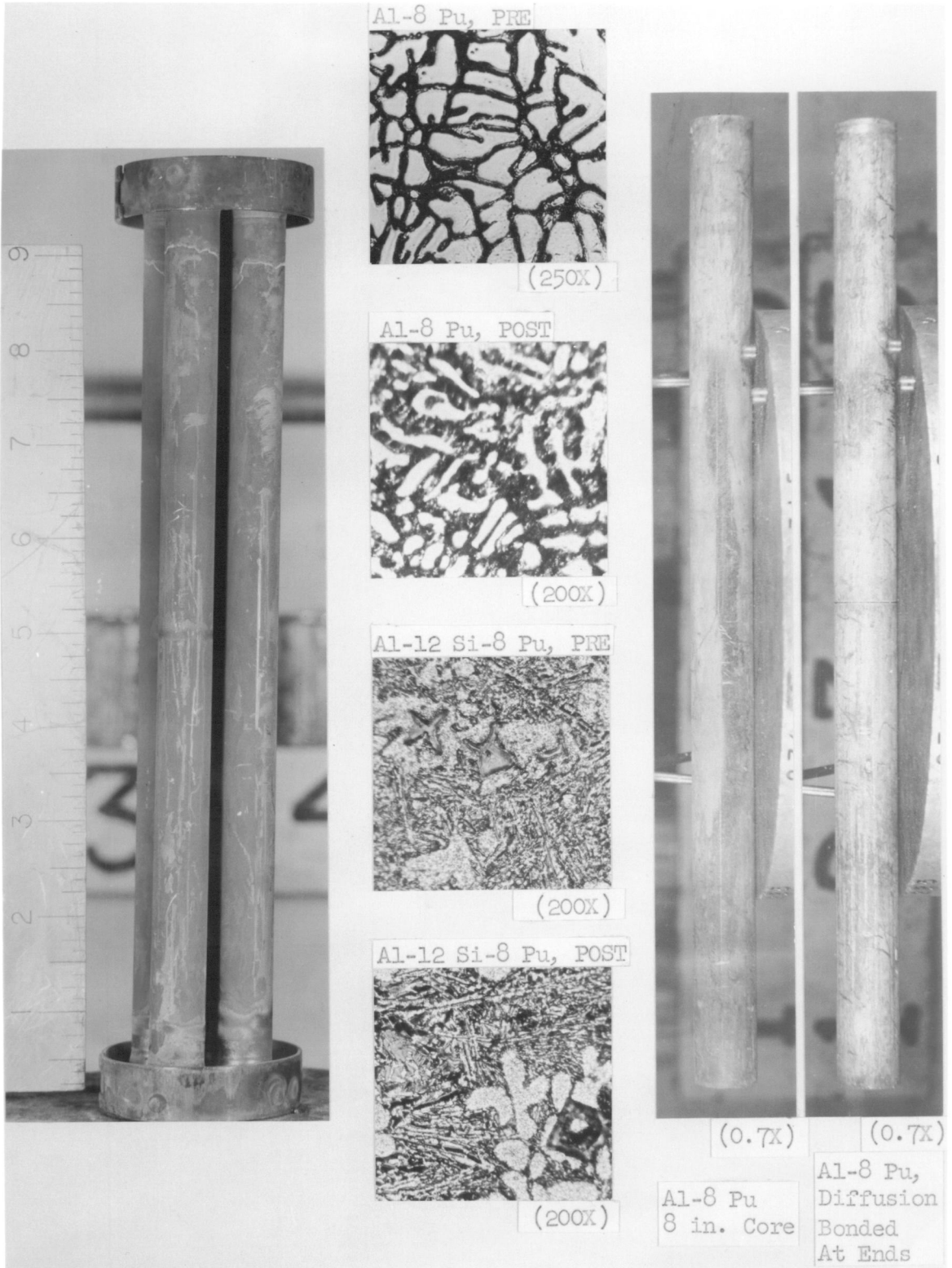


Fig. 13 - Irradiated, Zircaloy-Clad, Al-8 Pu and Al-12 Si-8 Pu Alloy, Four-Rod Cluster.

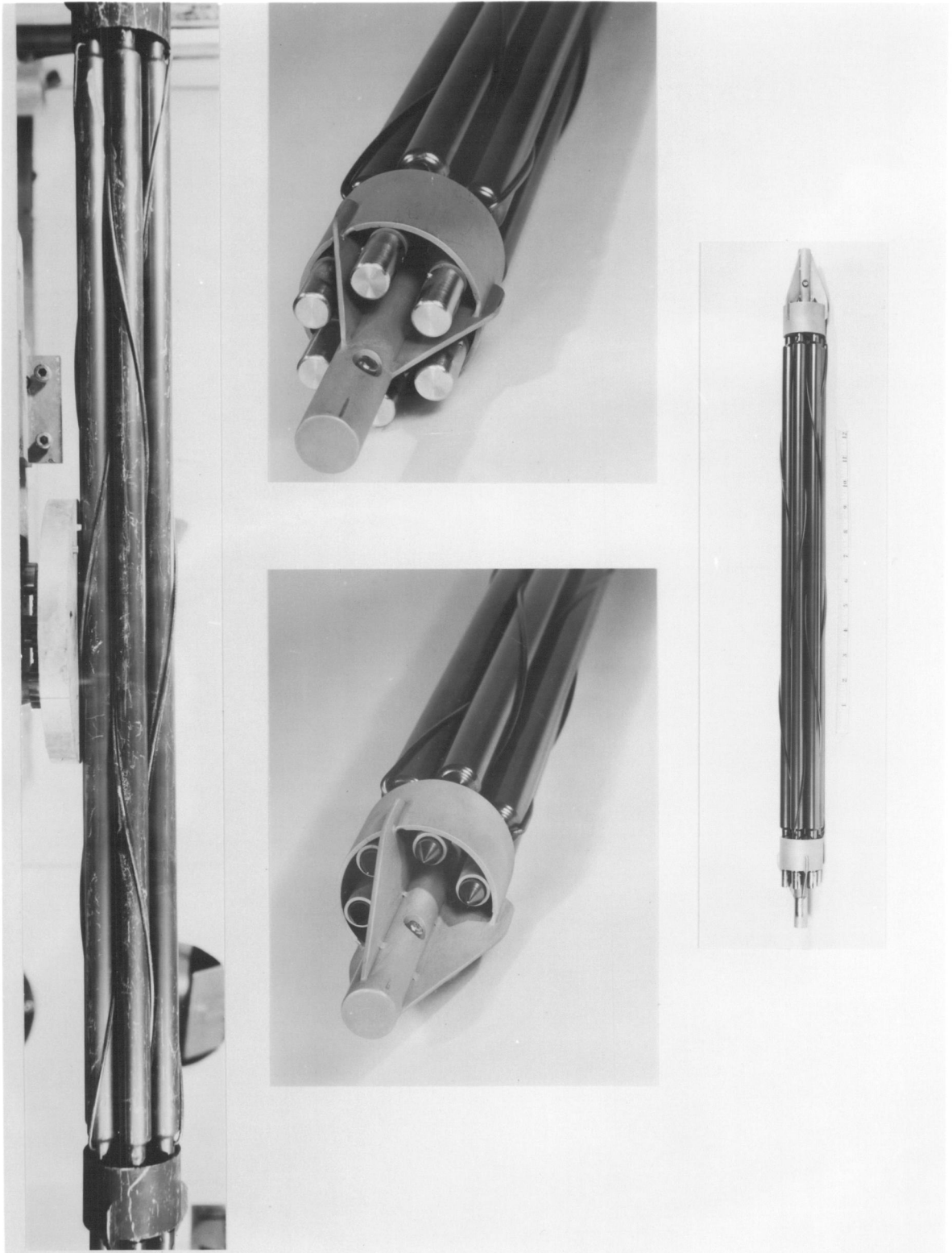


Fig. 14 - Irradiated, Zircaloy-Clad, Al-1.8 Pu Alloy Seven-Rod Cluster.

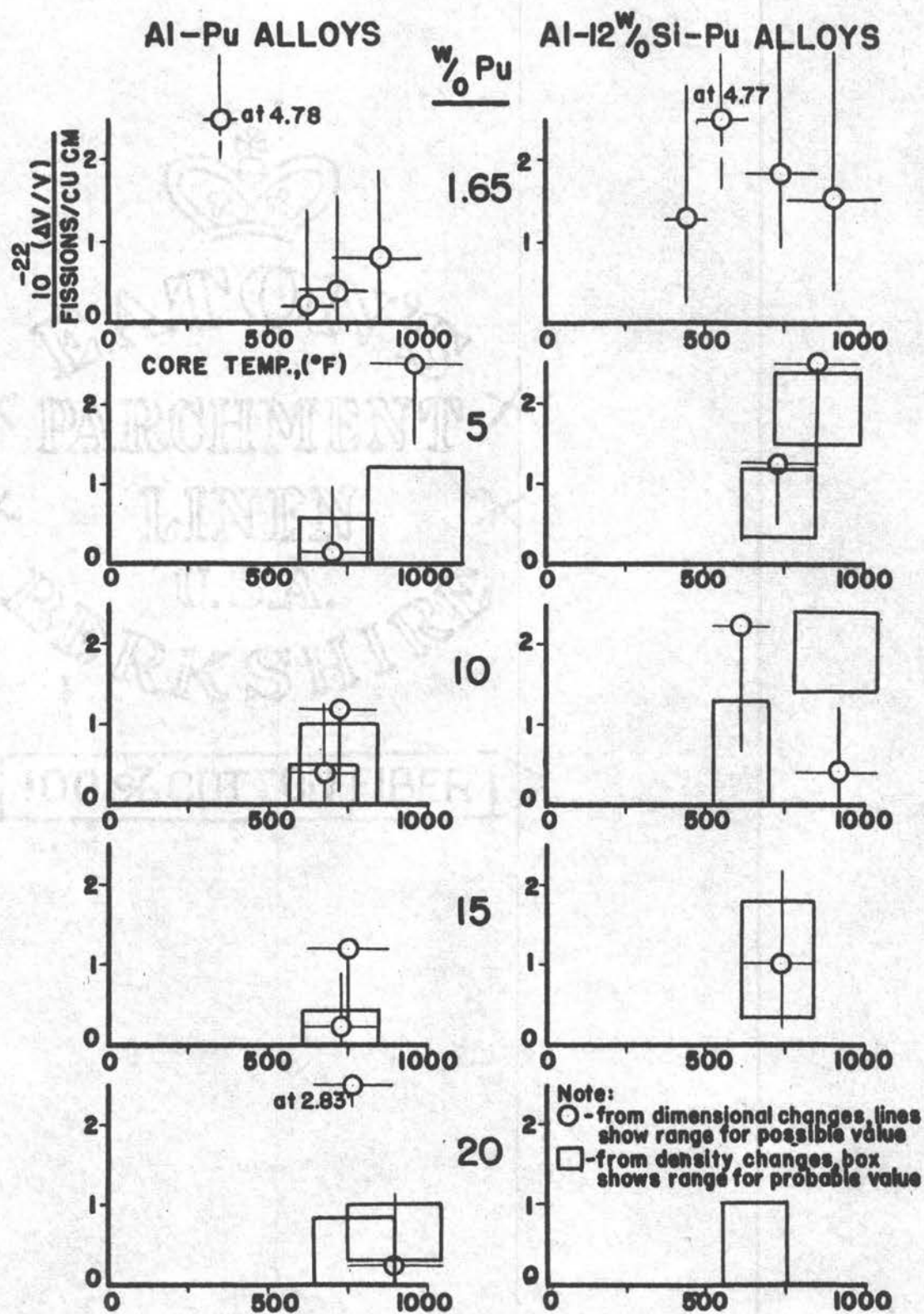


Fig. 15 - Graph of Ratio of Core Volume Change to Fissions Per Cubic Centimeter as a Function of the Calculated Fuel Core Temperature for Al-Pu and Al-Si-Pu Alloys.

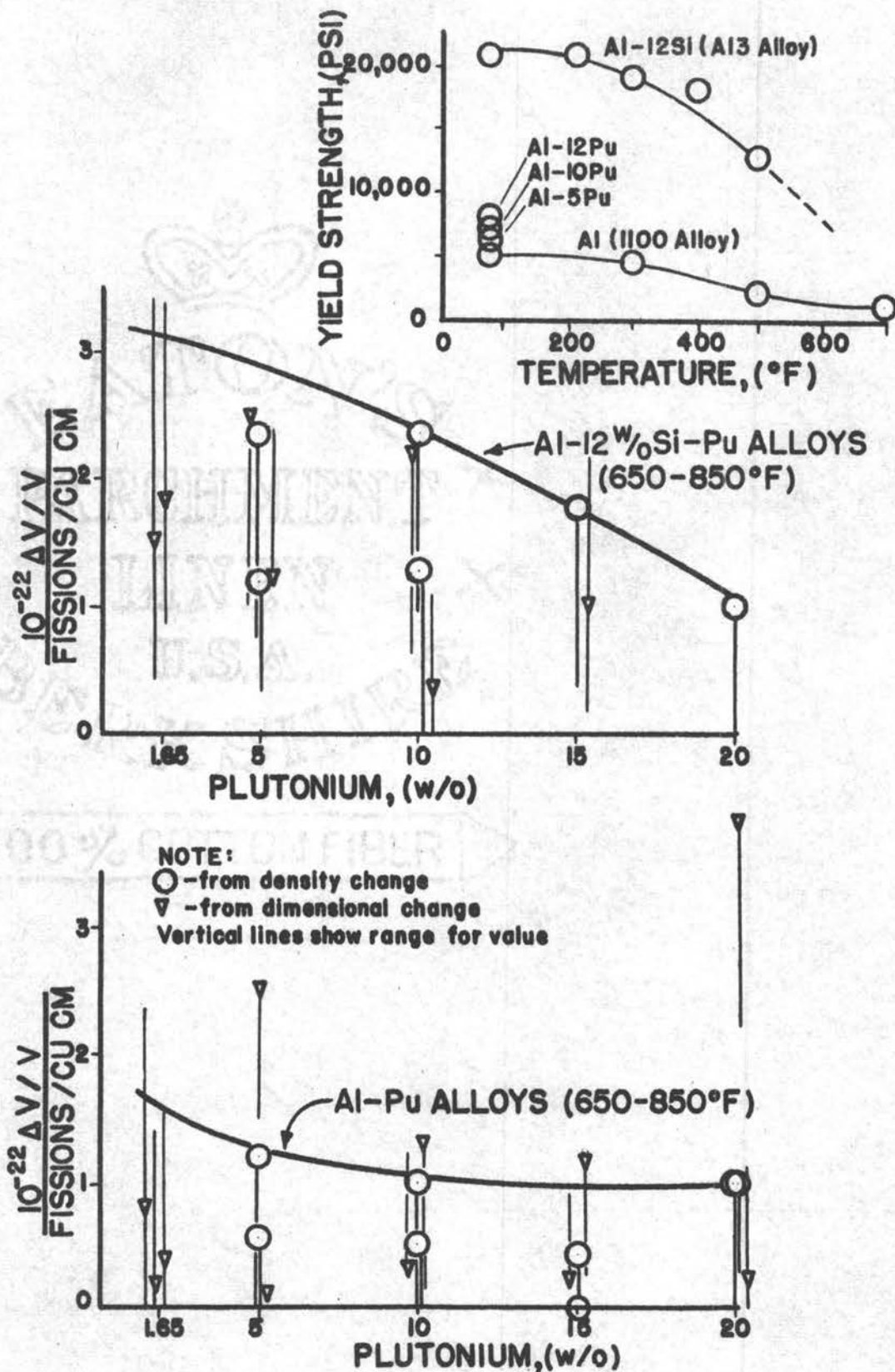


Fig. 16 - Graph of Ratio of Core Volume Change to Fissions Per Cubic Centimeter as a Function of Plutonium Concentration for Al-Pu and Al-Si-Pu Alloys in the Temperature Range 650-850 °F.

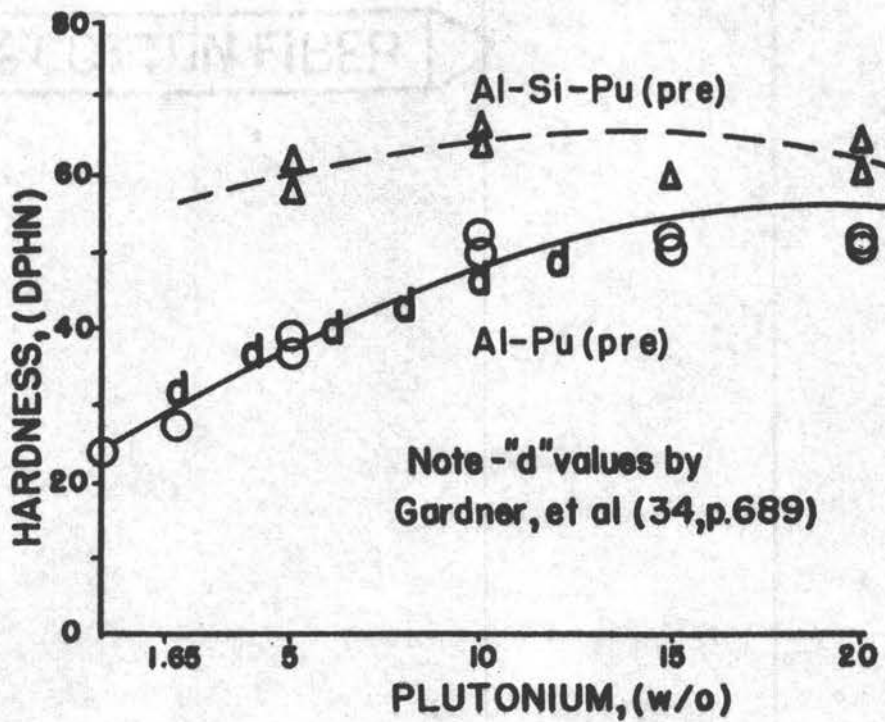
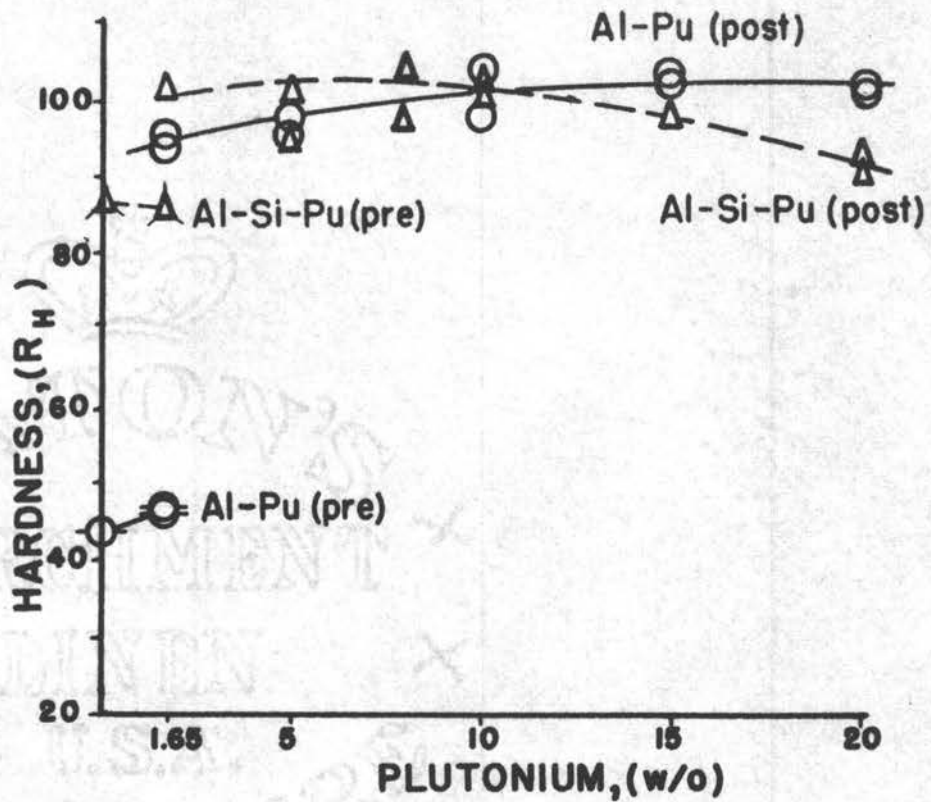
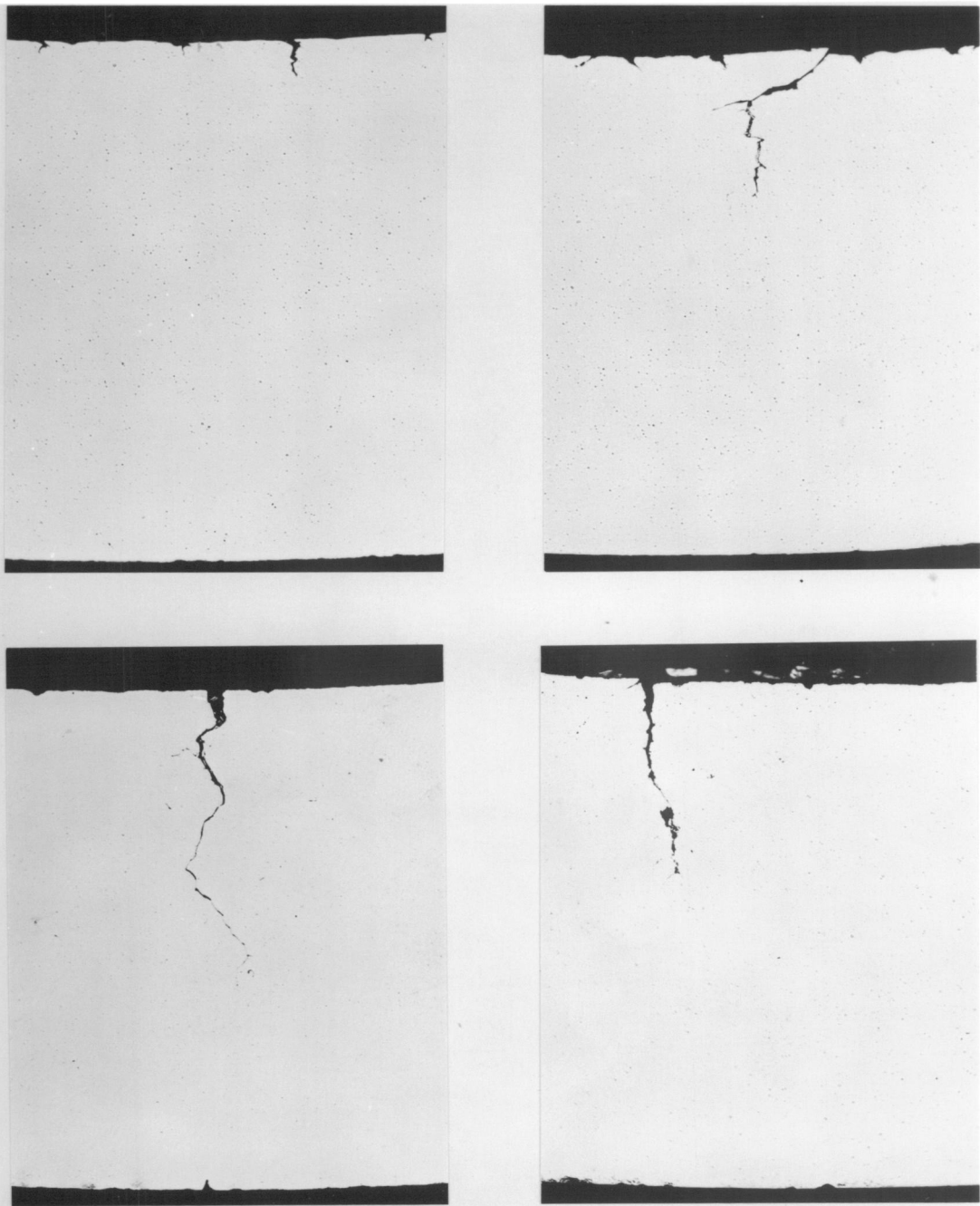


Fig. 17 -- Pre-and Post-Irradiation Hardness measurements on Al-Pu and Al-Si-Pu Alloys.



(100 X)

Fig. 18 - View of Typical Defects Observed in a Sample Lot of Zircaloy-2 Tubing.

Table XIII - Hardness Determinations on Al-Pu and Al-Si-Pu Alloys

Alloy Specimen	Specimen Number	Hardness (measured values underlined),			
		Pre-Irradiation		Post-Irradiation	
		A	E	H	K
Al (1100)			29	<u>44</u>	
Al-1.65 Pu	3-24-11			<u>46</u>	22 68 <u>94</u>
Al-1.65 Pu	14-23			<u>46</u>	<u>24</u> 72 96 43
Al-12 Si			<u>57</u>	87	
Al-12 Si-1.65 Pu	3-24-5		<u>55</u>	86	32 <u>82</u> 102
Al-12 Si-1.65 Pu	14-26		56	<u>86</u>	20 <u>42</u> 97 77
Al-8 Pu	186A-1				25 <u>73</u> 97
Al-12 Si 8 Pu	186A-8				34 <u>85</u> ~105

		<u>DPH Number</u>	<u>H</u>
Al (1100)		<u>24</u>	
Al-5 Pu	14-8	<u>39</u>	<u>96</u>
	14-45	<u>37</u>	<u>98</u>
Al-12 Si-5 Pu	14-6	<u>58</u>	<u>95</u>
	14-48	<u>62</u>	<u>101</u>
Al-10 Pu	14-5	<u>52</u>	<u>99</u>
	14-43	<u>50</u>	<u>104</u>
Al-12 Si-10 Pu	14-11	<u>67</u>	<u>103</u>
	14-47	<u>65</u>	<u>103</u>
Al-15 Pu	14-9	<u>52</u>	<u>103</u>
	14-44	<u>51</u>	<u>103</u>
Al-12 Si-15 Pu	14-7	<u>60</u>	<u>98</u>
	14-46		
Al-20 Pu	14-10	<u>52</u>	<u>103</u>
	14-42	<u>64</u>	<u>102</u>
Al-12 Si-20 Pu	14-12	<u>60</u>	<u>93</u>
	14-49	<u>65</u>	<u>90</u>

Table XIII - Examination Results for a Sample Lot of 71 Zircaloy-2

<u>Test</u>		<u>Test Section Length, (in.)</u>	<u>Tubes of Lot which Pass Test, (%)</u>
(A)	Eddy-current, OD	90	100
	ID	90	68
(B)	Fluorescent Penetrant, OD	90	45
	ID	90	4
(C)	Ultrasonic Flaw**		
	All Flaws < 0.009 in. deep	90	22
	All Flaws < 0.005 in. deep	90	15
(D)	Fluorescent Penetrant, OD	4	93
	ID	4	3
(E)	Flattening	0.5	54
(F)	Flare	1	58
(G)	Metallography		
	All Flaws < 0.009 in. deep	---	94
	All Flaws < 0.005 in. deep	---	62
	All Flaws < 0.003 in. deep	---	25
All Flaws < 0.0005 in. deep***	---	6	
(H)	Surface Finish (63 microinch, rms, min.)	1	74
(I)	Corrosion		
	Weight Gain ≤ 22 mg/(sq dm)	1	100
(J)	Wall Thickness		
	0.027 in. ≤ Wall ≤ 0.033 in.	90	92
(K)	Ult. Tensile Strength		
	Over 70,000 psi	8	26
	Over 65,000 psi	8	51
	Over 60,000 psi	8	96

* Zircaloy-2 Tube Data: ID = 0.505 - 0.510 in. Wall = 0.027 - 0.033 in. Length = 8.5 - 9.0 ft., Type = Seamless, Extruded.

** Number of Flaw Indications
 Tubes (%) 0/22 1/7 2-5/20 6-10/10 11-100/29 101-500/12

*** Number of Defects > 0.0005 in.
 Tubes (%) 0-2/10 3-10/30 11-20/37 21-30/13 31-40/10

of the 38 alloy cores. On the irradiated Al-Pu and Al-Si-Pu alloy specimens examined metallographically, no significant microstructural damage was noted. Some of the photomicrographs may be seen in Figures 6, 7, 9 and 13. Hardness measurements were made on a few of the samples and the results, some of which have been published (33, p.702-703), are shown in Figure 17 and Table XII. It appears that the rate at which hardening occurs tends to decrease with increasing exposure. This trend agrees with the literature (21, p. 483-484). Diffusion bonding of adjacent ends of two of the Al-8 Pu alloy fuel cores occurred in Rod 8 of the IP 186A cluster (Figure 13). No core-clad diffusion was observed. Metallographic examination indicated that the bonding was intermittent. The bond was strong enough, however, to permit transverse and longitudinal sectioning of the rod. In regard to core-clad diffusion, only one case has been noted to date in the alloy core specimens in the ten experiments. In Capsule GEH-14-49 of the third experiment, the presence of a mechanical or metallurgical bonding at one of the core-end cap interfaces was noted during the dejection operation in the radiometallurgical laboratory. The specimen operated at a calculated temperature of 890°F (477°C) as shown in Table V. There is a definite possibility of diffusion bonding at this temperature with Al or Al-Si alloys and Zircaloy (48, p. 1168).

Replicas were obtained from some of the specimens which had been examined metallographically. Because of the lack of suitable cathodic etching facilities, the metallographic samples were chemically etched prior to the replication step. The replicas were inspected by Bierlein

and Mastel on the electron microscope, and though precise interpretation of the results was impossible due to the etching treatment of the original sample, it was indicated that no marked microstructural damage was observable. By an autoradiographic technique, they were able to clearly show the location of the plutonium in the irradiated Al-1.65 Pu and Al-12 Si-1.65 Pu alloy fuel cores as shown in Figure 9. As theory predicts and as Figure 9 shows, the relatively hard and brittle intermediate phase, PuAl_4 , is found in the interstices of the primary dendrites. It has been reported (53, p. 26) that the solid solubility of plutonium in aluminum, if not zero, is too low to be determined by the lattice constant method. Recent data by Pallmer and Hall (70, p. 5, 8) indicate a solid solubility of plutonium in aluminum of 0.26 - 0.5 percent at 600°C . The specimen in Figure 9 does not exhibit visual evidence of plutonium within the dendrites.

It should be stated that the Al-Pu alloy phase diagram and the alloy microstructures show the existence of a eutectic composition at 86.7 weight percent (98.3 atomic percent) aluminum. This eutectic structure has been found to exist in all Al-Pu alloys containing more than about 80 percent aluminum (53, p. 35). There is no known phase diagram available at this time for the Al-12 Si-Pu alloy system. Bloomster has experimentally established a number of points in the system and has indicated that in the 1.65 - 20 percent Pu range, the plutonium is probably present in the form of a Pu-Si intermediate phase (76, Jan.-Mar., 1960).

Examination of the photomicrographs in Figure 6 reveals the

presence of the primary aluminum dendrites (light phase) and the Al-PuAl₄ eutectic (dark phase) in the hypo-eutectic, Al-Pu alloys. In the case of the hyper-eutectic alloys, one observes primary PuAl₄ (diamond-shaped phase), eutectic (lamellar phase), and aluminum (light phase). In the case of the Al-Si-Pu alloys in Figure 7, the plutonium has been added to an Al-Si alloy of the eutectic composition. For the Al-Si-Pu alloys, the solidus temperature is believed to vary approximately linearly from 1068°F (575°C) for Al-12 Si alloy to 1112°F (600°C) for the Al-12 Si-20 Pu alloy.

Dimensional measurement on the clad and unclad alloy fuel cores were obtained and the volumetric changes calculated (Tables II-IV and X). Density determinations were made on the alloy cores shown in Tables IV and V. The density changes are believed to be a more accurate measure of the volumetric changes which have occurred. The relationship between the composition, volume change, temperature, and exposure (measured in fissions per cubic centimeter) is graphically presented in Figures 15 and 16. From the graphical and tabular data, the following observations on the Al-Pu and Al-12 Si-Pu alloy specimens tested were made. The percentage change in fuel core volume tends to increase with increasing fuel core temperature and the percentage change in fuel core volume is more sensitive to fuel temperature than to exposure (measured in fissions/cu cm). It appears from the graphs in Figure 16 that for the temperature range 650 - 850°F (344-454°C) the Al-Pu alloys are more resistant to deformation than the Al-Si-Pu alloys with the same plutonium content. In both alloy cases, the re-

sistance to deformation increases with increasing plutonium content. If one considers the melting points of the two alloy systems and compares the performance of the alloys at a fixed percentage of their melting points, it is found that in general the Al-Si-Pu alloys are quite comparable to the Al-Pu alloys. The plot of yield strength versus temperature in Figure 16 shows that although the Al-Si alloy is much stronger at room temperature, the yield strength drops off very rapidly and approaches that of Al (1100 alloy) at 700°F. In Figure 15, the two markedly different points in the Al-Pu and Al-Si-Pu alloys with 1.65 weight percent plutonium may possibly be explained by one or more of the following reasons. In both cases the number of fissions/cu cm is much lower (about 1/2 to 1/3) than the value for all of the other points. The specimens in Experiments 1 and 2 were not annealed as were all other alloy capsule cores. It is possible that the observed volume change is due in part to residual stresses and since the exposure is much lower than that of other capsules, the value for the volume change divided by fissions/cu cm would be significantly increased.

It is possible that the dimensional changes are due in part to a thermal ratcheting phenomenon since there is a marked difference (factor of about four) in the coefficient of thermal expansion between the fuel alloy and the Zircaloy. For the same core temperature, it was noted that the Al-Si-Pu alloys in general appear to exhibit a larger volume change. An interesting item is that thermal cycling tests of aluminum and Alpax (Al-13.0 Si-0.35 Fe) between 68 and 932°F show that the volume changes after 180 cycles were 14 and 6 percent,

respectively (12, p. 290). It was also found that for the temperature range 20-300°C and a holding period of ten minutes, the length change in pure aluminum was 1.4 percent for 50 cycles and 2.9 percent for 100 cycles. It appears that in the irradiated capsules, some restraint was exerted by the cladding on the cores. Inspection of the tabular data for the Al-Pu and Al-Si-Pu alloys indicates the following trends:

<u>Thermal Cycles</u>	<u>Temperature</u>	$\frac{\Delta V/V}{\text{Fissions/cu cm}}$	$\frac{\Delta L}{\text{Core}}$	$\frac{\Delta L}{\text{Clad}}$
(1) Increase	+ Increase	= Increase	+ Increase	+ Increase
(2) Decrease	+ Increase	= Decrease	+ Decrease	+ Decrease

The phenomenon of directional residual deformation depends to great extent on the following variables: upper temperature of the cycle and the heating and cooling rates; also to some extent on the exposure duration at the upper temperature of the cycle (12, p. 290).

The alloy-core capsules and the four-rod cluster (Figure 13) demonstrated that unless extraordinary reactor conditions were encountered or the fuel core and cladding were damaged during handling operations subsequent to irradiation, that the fuel cores were readily removed from the jackets. As anticipated, the ease of core removal was an inverse function of exposure.

The seven-rod cluster (IP 226A), discharged after successfully receiving an exposure of 4.7×10^{20} nvt, is currently undergoing radio-metallurgical examination. A preliminary visual inspection of the irradiated element at the reactor storage basin indicated that no gross deformation occurred and this has been confirmed in the hot cell. The specimen is shown in Figure 14. The stainless steel end brackets are

now about the same color as the autoclaved Zircaloy.

In general, it was concluded and reported (33, p. 702-703) that the performance of the alloy specimens was good and dimensional changes were not deleterious. The satisfactory irradiation behavior of the Al-Pu alloys agrees with the experience reported by other investigators (68, p. 60) (73, p. 360).

Well after the irradiation testing program was initiated, high temperature and pressure autoclaves were obtained and installed for corrosion testing materials containing plutonium. Actual data on the high-temperature, aqueous corrosion of Al-Pu and Al-12 Si-Pu alloys with 1.8-15 weight percent Pu have been obtained and reported by Bowen (15, p. 1-8). The tests were short term (one day or less), were performed in 350°C and 360°C water, and employed both as-cast and extruded alloy specimens. Because the Al-1.8 Pu alloy performed poorly corrosion-wise and since the Al-12 Si-Pu alloys present severe separation problems (72, p. 1-13), exploratory work was commenced in order to develop a more corrosion resistant alloy to replace the Al-Pu alloy. Recent tests by Bloomster and Katayama (76, Jan. - Mar., 1960) indicate that bare specimens of an alloy with the composition Al-1.8 Pu-1.35 Ni-1.10 Si-0.35 Fe possess good resistance to corrosive attack in 350°C water for periods up to 24 hours. This alloy has since been adopted for the actual fuel cores in the initial PRTR spike assemblies (27, p.3) (76, Jan.-Mar., 1960). No intentionally defected elements containing Al-Pu or some modification of this alloy have been irradiated to date.

The UO_2 - PuO_2 capsules have been and are being irradiated and a

limited amount of radiometallurgical examination has been performed to date. The data for the oxide pieces is shown in Tables VI-IX and the photographs may be seen in Figures 10-12. All specimens were visually inspected and measured. No significant dimensional changes in the capsule cladding were noted.

In comparison to the pre-irradiated sample, the irradiated specimen GEH-14-19 exhibited a noticeable but expected grain difference. Chikalla estimated that the average grain size in the central area to be about four to five times greater on the irradiated specimen and that at the edge of the pellets, the average grain area was approximately the same for both samples (1, p. A21). No central void was formed. The irradiated specimen displayed large, radially-oriented grains in the center of the transverse section. The appearance was very typical of irradiated UO_2 - PuO_2 samples and was quite similar to irradiated UO_2 . The performance of this material compares favorably with the experience reported by other investigators (16, p. 1-33) (43, p. 1-22) (11, p. 2-25) (74, p. 327) (52, p. 9).

Capsule GEH-14-21 was pressurized to about two atmospheres and when punctured, released approximately 11 milliliters of gas. The specimen contained a central void and it may be observed in Figures 11 and 12. In situ reactor sintering was anticipated and did occur. Note the large, radially oriented columnar grains shown in Figure 12.

Capsule GEH-14-65, shown in Figures 11 and 12, shows possible indications of center core melting. Note the porous center section, the irregular inner surface of the outer section, the very dense large

grains and the apparently unsintered material at the outer boundary. It is estimated that the core temperature was on the order of 2000-2700°C. To effect such a change in the microstructure, it is believed that a phase change must occur. This change could be accomplished by vaporization-sublimation or by melting.

From the data in Tables VI-IX, it appears that the higher density material definitely retains more of the fission gas. It is of interest to note that the highest gas release values occurred in the low density pieces with the smallest PuO₂ additions.

It was reported that with UO₂ pellets with densities of 91 and 65 percent of the theoretical value, that the fission gas release was 3 and 40 - 50 percent, respectively (23, p. 543). The fission gas products should have a composition of about 15.3 percent krypton and 84.7 percent xenon. The lighter krypton is more readily set free from the crystal lattice so one should expect the krypton/xenon ratio in the released fission gas to be in general in excess of 0.18. The gas release values stated for the test capsules in Tables VI-IX are not completely reliable in that air in-leakage has been detected in the gas sampling system. The grain growth observed in the test capsules agrees with experimental data which has been reported (20, p. 524). The authors reported grain growth in UO₂ capsules with diametral clearances of 0.001 - 0.004 inches which were irradiated under conditions to give heat fluxes up to 430,000 Btu/(hr)(sq ft).

The test element which has failed to date is GEH-14-89 (Figure 12). The capsule contained high-density, UO₂-PuO₂ pellets and had been

irradiated for two cycles (about 30 days) in the MTR. It was examined, found to be in good condition, and was reinserted into the reactor. It was advertantly placed in a neutron flux eleven times higher than the specified value. The element remained in the position for six days before it was discharged. Increased coolant activity was noted on the second day and the activity continued to climb until it reached the allowable limit. After discharge, the capsule was examined. No fuel remained. An extensive core-end cap reaction had occurred. Hydride formation was observed during the hot cell examination. Gross cracking of the cladding in the rupture site vicinity was noted.

The sample lot of 93 Zircaloy-2 tubes, selected from an initial group of tubes purchased for jacketing material for fuel element clusters was extensively examined. The results obtained to date on 71 pieces from the sample lot are shown in Table XIII. The examinations were performed by O'Claire (Tests A-D, F and J), by Hartcorn (Test G), and by Shannon (Test I). Tests completed to date indicate a high incidence of cracking, with cracks from 0.001 - 0.020 inches in depth as shown in Figure 18. All of the cracks or defects appear to be in the direction of the longitudinal tube axis. The defects observed to date are from about 1/16-inch to 11 inches in length. Examination of the sample-lot test results indicated that the probability of any given tube containing one or more defects 0.005 inches or greater in depth approached 100 percent. A major share of the evaluation work was performed by Bardsley (76, Oct.-Dec., 1959). Of the tests outlined in Table XIII, it has been found and reported (76, Jan.-Mar., 1960) that

the ultrasonic flaw test was the most satisfactory method for efficiently sorting out tubes with undesirable defects. On the samples examined metallographically, it was found that the hardness and grain size was uniform and the same in both the defective and good tubes. Microscopic examination for the presence of hydrides was made at 250X. In comparison to a standards chart, the samples showed a hydride concentration of less than 8 ppm. Tensile strength data revealed no apparent trend. The corrosion tests were conducted for 72 hours in steam at 400°C and 1500 psig.

Recent ultrasonic flaw tests on 403 tubes showed that 93 percent contained defects 0.005 inches or greater in depth and confirm the prediction made from the sample lot tests. The standard for the ultrasonic flaw testing of tubes has defects in the inner surface which have been calibrated by means of metallography. The 0.009 inch deep crack in the standard was used to locate a flaw in a tube which would produce approximately the same pattern on the oscilloscope screen. Metallographic examination by Hartcorn (76, Jan-Mar., 1960) of the 1/2-inch defect in the tube ID revealed the following information:

<u>Distance from One End of Detected Flaw, (in)</u>	<u>Defect Depth, (in)</u>
0	0.0035
1/16	0.0059
1/8	0.018
3/16	0.0072
1/4	0.0024
5/16	0.0016
3/8	0.0014
7/16	0.0001
1/2	0.0000

Through examination of the adjacent tube sections it was found that a defect at least 0.012 inches deep could appear and disappear in 1/16 inch of tube length.

It was concluded from the limited number of experiments and observations made to date that:

- (a) Al-Pu alloys with 1.65-20 Pu exhibit very good irradiation behavior in the temperature, power generation, heat flux, and exposure ranges of interest to the PRTR.
- (b) Al-12 Si-Pu alloys with 1.65-20 Pu perform satisfactorily in the reactor in the desired range of fuel element operating variables but are not being contemplated for actual PRTR usage because of the severe separations problem.
- (c) The Al-Pu alloys display relatively poor corrosion resistance to high pressure and temperature water. The alloy which shows a marked improvement in corrosion properties and which is now specified for the initial PRTR spike-enrichment loadings is Al-1.80 Pu-1.35 Ni-1.10 Si-0.35 Fe.
- (d) If the Al-Pu and Al-12 Si-Pu alloys are compared on the basis of (volume change)/(fissions/cu cm) as a function of plutonium concentration (1.65-20 weight percent) and for a fuel core temperature of 650-850°F, it is found that the Al-Pu is better by nearly a factor of two. In addition, in both alloy cases the resistance to deformation increases with increasing plutonium content.
- (e) For the Al-Pu and Al-Si-Pu alloys studied, the percentage

change in fuel core volume tends to increase with increasing fuel core temperature and the percentage change in fuel core volume is more sensitive to fuel temperature than to exposure.

- (f) The cluster experiments indicate that the element design is satisfactory and will perform well in high pressure and temperature coolant.
- (g) The high-density, UO_2 - PuO_2 pellets with 0.0259 - 5.67 atomic percent PuO_2 made with mixed crystal oxides or a mechanical mixture of the oxides have shown good in-reactor operation and low fission gas release rates for exposures of 1000-2000 MWD/T.
- (h) The non-sintered, low-density, UO_2 - PuO_2 pellets fabricated with 0.0259 - 7.45 atomic percent PuO_2 have shown good reactor performance. Mixed crystal oxides and mechanical mixtures of the plutonium and uranium oxides were used. In situ reactor sintering occurred and a central void was formed in two of the capsules which have been sectioned and examined to date. More work needs to be done with this element to insure safe and reliable performance. The elements sectioned had exposures of 1000-2000 MWD/T. Elements are currently being tested to higher exposures.
- (i) No significant difference has been detected between the irradiated UO_2 - PuO_2 capsules made with the mixed crystal oxides and with the mechanical mixtures.

- (j) The degree of cracking of the UO_2 - PuO_2 cores appears to decrease with increasing PuO_2 content in the limited number tested and examined to date.
- (k) The extruded Zircaloy tubing for PRTR fuel elements must be carefully scrutinized for flaws, especially on the interior surface. Extensive testing work indicates that an ultrasonic flaw test is one of the more effective methods for sorting out reject tubes.

BIBLIOGRAPHY

1. Albaugh, Fredrick W. 1960. 50p. (U. S. Atomic Energy Commission. HW-64108A. Classified)
2. Albaugh, Fredrick W. Plutonium recycle program monthly reports, Reactor and Fuels Research and Development Operation, General Electric Company, Hanford Atomic Products Operation, Richland, Washington,
 - HW-50339A2, May, 1957. 14p.
 - HW-51234A2, June, 1957. 12p.
 - HW-51741A2, July, 1957. 16p.
 - HW-52303A2, August, 1957. 21p.
 - HW-52859A2, September, 1957. 18p.
 - HW-53299A2, October, 1957. 20p.
 - HW-53961A2, November, 1957. 14p.
 - HW-54284A2, December, 1957. 19p.
 - HW-54760A2, January, 1958. 21p.
 - HW-55162A2, February, 1958.
 - HW-55590A2, March, 1958. 18p.
 - HW-55905A2, April, 1958.
 - HW-56185A2, May, 1958. 17p.
 - HW-56640A2, June, 1958. 16p.
 - HW-56914A2, July, 1958. 15p.
 - HW-57225A2, August, 1958. 18p.
 - 1957-1958. (U. S. Atomic Energy Commission. HW-50339A2, 51234A2, 51741A2, 52303A2, 52859A2, 53299A2, 53961A2, 54284A2, 54760A2, 55162A2, 55590A2, 55905A2, 56185A2, 56914A2, 57225A2)
3. American Society for Testing Materials. Symposium on non-destructive tests in the field of nuclear energy. Baltimore, 1958. 395p. (ASTM Special Technical Publication no. 223)
4. Atwood, John M. and Wayne A. Snyder (eds.). Plutonium recycle program annual report fiscal year 1959. 1959. 138p. (U. S. Atomic Energy Commission. HW-62000)
5. Bailey, Wendell J. et al. Fabrication of aluminum-plutonium alloy fuel elements by coextrusion. 1959. 30p. (U. S. Atomic Energy Commission. HW-63151)
6. Bailey, Wendell J. 1958. 21p. (Atomic Energy Commission. HW-56680. Classified)
7. Bailey, Wendell J. 1957. 9p. (Atomic Energy Commission. HW-53510. Classified)

8. Bailey, Wendell J. 1957. 6p. (Atomic Energy Commission. HW-53511. Classified)
9. Bailey, Wendell J., Richard K. Koler, and David A. Patterson. Fabrication of aluminum-plutonium fuel elements for lattice tests in support of PRTR. 1958. 32p. (U. S. Atomic Energy Commission. HW-51855)
10. Bagley, K. Q. Plutonium-and its alloys. Nuclear Engineering 2:461-468. Nov. 1957.
11. Bates, J. Lambert and William E. Roake. Irradiation testing of plutonium-uranium oxide nuclear fuel. 1959. 25p. (U. S. Atomic Energy Commission. HW-61142)
12. Bochvar, A. A. et al. Effect of thermal cycling on dimensional stability of various metals and alloys. In: International conference on the peaceful uses of atomic energy, Geneva, 1958. Proceedings. Vol. 5. Switzerland, United Nations Publication, 1958. p.288-299. (Paper p/2190)
13. Bonilla, Charles F. (ed.) Nuclear Engineering. New York, McGraw-Hill, 1957. 850p.
14. Bowen, Harry C. and Robert L. Dillon. Intergranular corrosion of aluminum-uranium and aluminum-silicon-uranium alloys. 1958. 11p. (U. S. Atomic Energy Commission, HW-55352)
15. Bowen, Harry C. High temperature aqueous corrosion of aluminum-plutonium and aluminum-silicon-plutonium alloys. 1959. 11p. (U. S. Atomic Energy Commission. HW-61345)
16. Cashin, W. M. 1955. 33p. (U. S. Atomic Energy Commission. KAPL-1446. Classified)
17. Chikalla, Thomas D. Sintering studies on the system UO_2 - PuO_2 . I. Solid solution formation. 1959. 13p. (U. S. Atomic Energy Commission. HW-60276)
18. Chikalla, Thomas D. Sintering studies on the system UO_2 - PuO_2 . II. Sinterability. 1959. 38p. (U. S. Atomic Energy Commission. HW-60381)
19. Chikalla, Thomas D. Studies on the oxides of plutonium. 1959. 51p. (U. S. Atomic Energy Commission. HW-63574)

20. Cohen, P. and D. M. Wroughton. Requirements and techniques for irradiation testing of reactor materials for pressurized water reactors. In: International conference on the peaceful uses of atomic energy, Geneva, 1958. Proceedings. Vol. 7. United States of America, United Nations Publication, 1958. p.499-530. (Paper p/2508)
21. Cottrell, A. H. Effects of neutron irradiation on metals and alloys. In: Metallurgical Reviews. Vol. 1. London, Institute of Metals, 1956. p.479-522.
22. Dienes, G. J. Displaced atoms in solids-comparison between theory and experiment. In: Symposium on radiation effects on materials. Vol. 1. Baltimore, American Society for Testing Materials, 1958. p.3-26. (ASTM Special Technical Publication no. 208)
23. Dietrich, Joseph R. and Walter H. Zinn. Solid Fuel Reactors. Reading, Addison-Wesley, 1958. 844p.
24. Doman, D. R. Out-of-reactor tests on Pu-Al type PRTR elements for 1706-KER testing. 1959. 10p (U. S. Atomic Energy Commission. HW-61417)
25. Farnsworth, P. L. and G. R. Horn. Detection and evaluation of Zircaloy-2 tubing defects. 1959. 17p. (U. S. Atomic Energy Commission. HW-61935)
26. Forscher, F. Mechanical properties evaluation of Zircaloy-3. 1956. 47p. (U. S. Atomic Energy Commission. WAPD-143)
27. Fox, John C. and Marlyn T. Jakub. Unpublished document on PRTR engineering data November 18, 1959. Richland, Washington, Design Development Operation, General Electric Company, Hanford Atomic Products Operation. 1959. 15p.
28. Freshley, Maxwell D. and Fred E. Young. Proposal for irradiating an aluminum-plutonium nineteen rod cluster. (GEH-11-2) in the ETRC69G7 Facility. 1959. 18p. (U. S. Atomic Energy Commission. HW-60371)
29. Freshley, Maxwell, D. and Fred E. Young. Proposal for irradiating an aluminum-plutonium seven rod cluster (GEH-11-1) in the ETR7P33 facility. 1959. 19p. (U. S. Atomic Energy Commission. HW-60155)

30. Freshley, Maxwell D. GEH-4-46, three rod cluster aluminum-plutonium alloy swaged element irradiation. 1959. 12p. (U. S. Atomic Energy Commission. HW-62191)
31. Freshley, Maxwell D. GEH-4-43, three rod cluster aluminum-plutonium alloy slip fit element irradiation. 1959. 13p. (U. S. Atomic Energy Commission. HW-62839)
32. Freshley, Maxwell D. Plutonium-aluminum fuel element development. 1957. 44p. (U. S. Atomic Energy Commission. HW-52457)
33. Freshley, Maxwell D., Thomas C. Nelson, and Oswald J. Wick. Plutonium fuels development. In: International conference on the peaceful uses of atomic energy, Geneva, 1958. Proceedings. Vol. 6. Great Britain, United Nations Publication, 1958. p.700-709. (Paper p/1776)
34. Gardner, Howard R., Clarence H. Bloomster, and James M. Jefferes. The tensile properties of pure plutonium and some aluminum-plutonium alloys. In: International conference on the peaceful uses of Atomic Energy, Geneva, 1958. Proceedings. Vol. 6. Great Britain, United Nations Publication, 1958. p.686-689. (Paper p/1081)
35. General Electric Company, Hanford Atomic Products Operation, Hanford Laboratories Operation. Annual report plutonium recycle program fiscal year 1957. 1957. 106p. (U. S. Atomic Energy Commission. HW-52000)
36. General Electric Company, Hanford Atomic Products Operation, Hanford Laboratories Operation. Plutonium recycling in thermal reactors. 1958. 112p. (U. S. Atomic Energy Commission. HW-55800)
37. Gibney, Robert B. Preliminary report on thermal and electrical conductivities of some plutonium-aluminum alloys. 1950. 10p. (U. S. Atomic Energy Commission. LAMS-1080. Declassified)
38. Goldsmith, S. Annual report, fiscal year 1958. 1958. 119p. (U. S. Atomic Energy Commission. HW-58000)
39. Goodwin, J. C. The effect of heat treatment on the corrosion resistance of Zircaloy-2 and Zircaloy-3. In: Bettis technical review. 1958. p.39-47. (U. S. Atomic Energy Commission. WAPD-BT-6)

40. Grass, R. C. and J. F. Hogerton (eds). General properties of materials. In: The Reactor Handbook. 1955. 3 vols. (U. S. Atomic Energy Commission. AECD-3647)
41. Hardy, H. K. and H. Lawton. The assessment and testing of fuel elements. In: International conference on the peaceful uses of atomic energy, Geneva, 1958. Proceedings. Vol. 5. Switzerland, United Nations Publication 1958. p.521-531. (Paper p/306)
42. Harrison, L. J. Operating parameters and neutron flux profiles for MTR plutonium core. 1959. 67p. (U. S. Atomic Energy Commission. IDO-16526)
43. Jens, W. H. 1954. 22p. (U. S. Atomic Energy Commission. NDA-14-42. Classified)
44. Kass, Stanley. Second interim report on the corrosion behavior of Zircaloy-3. 1956. 21p. (U. S. Atomic Energy Commission. WAPD-ALW-M-71)
45. Kratzer, William K. 1960. 27p (U. S. Atomic Energy Commission. HW-64444. Classified)
46. Lemon, Lloyd, C. End closure for plutonium bearing Zircaloy-2 clad fuel elements. 1959. 17p. (U. S. Atomic Energy Commission. HW-60910)
47. Lustman, B. Engineering aspects of radiation on nuclear fuels. In: Symposium on radiation effects on materials. Vol. 2. Baltimore, American Society for Testing Materials, 1958. p.84-105. (ASTM Special Technical Publication no.220)
48. Lyman, Taylor. Metals Handbook. 1948 ed. Cleveland, The American Society for Metals, 1952. 1332p.
49. McAdams, William H. Heat Transmission. 3d ed. New York, McGraw-Hill, 1954. 532p.
50. McEwen, Larry H. Reactor development program monthly reports Programming Operation, General Electric Company, Hanford Atomic Products Operation, Richland, Washington, HW-57636A2, September, 1958. 26p.
HW-58019A2, October, 1958. 25p.
HW-58555, November, 1958. 28p.
HW-58860, December, 1958. 36p.

HW-59179, January, 1959. 32p.
HW-59600, February, 1959. 30p.
HW-60043, March, 1959. 35p.
HW-60331, April, 1959. 31p.
HW-60674, May, 1959. 31p.
HW-61084, June, 1959. 37p.
HW-61575, July, 1959. 36p.
HW-61888, August, 1959. 39p.
HW-62362, September, 1959. 40p.
HW-62579, October, 1959. 39p.
HW-63070, November, 1959. 48p.
HW-63531, December, 1959. 47p.
HW-63936, January, 1960. 51p.
HW-64307, February, 1960. 56p.
March, 1960.
April, 1960.
May, 1960.
1958-1960. (U. S. Atomic Energy Commission. HW-57636A2,
58019A2, 58555, 59179, 59600, 60043, 60331, 60674, 61084,
61575, 61888, 62362, 62579, 63070, 63531, 63936, 64307)

51. Merckx, Kenneth R. (ed.) Fuel element design handbook, 1958. 81p. (U. S. Atomic Energy Commission. HW-51000. Declassified)
52. Minor, James E. 1959. 9p. (U. S. Atomic Energy Commission. HW-61309. Classified)
53. Moeller, R. D. and F. W. Schonfield, Alloys of plutonium and aluminum. 1950. 71p. (U. S. Atomic Energy Commission. LA-1000. Declassified)
54. Morrison, W. G. Thermal conductivity of gas mixtures in UO_2 fuel elements. 1957. 24p. (Atomic Energy of Canada Limited. NEI-88)
55. Muraoka, Jack. Design of tubular fuel elements for the PRTR. 1957. 12p. (U. S. Atomic Energy Commission. HW-53319)
56. Murray, P. and J. Williams. Ceramic and cermet fuels. In: International conference on the peaceful uses of atomic energy, Geneva, 1958. Proceedings. Vol. 6. Great Britain, United Nations Publication, 1958. p.538-550. (Paper p/318)
57. Neidner, Robert. GEH-14-82 through 91; high density UO_2 - PuO_2 capsule irradiation. 1959. 12p. (U. S. Atomic Energy Commission. HW-60694)

58. Neidner, Robert. GEH-14-5, 6, 7, 8, 9, 10, 11, and 12: Al-Pu alloy capsule irradiation. 1959. 7p. (U. S. Atomic Energy Commission. HW-59972)
59. Neidner, Robert. GEH-14-42, 43, 44, 45, 46, 47, 48, and 49: Al-Pu alloy capsule irradiation. 1959. 4p. (U. S. Atomic Energy Commission. HW-60692)
60. Neidner, Robert. GEH-14-19, 20: high density UO_2 - PuO_2 capsule irradiation. 1959. 11p. (U. S. Atomic Energy Commission. HW-59970)
61. Neidner, Robert. GEH-14-65 through 74: low density UO_2 - PuO_2 capsule irradiations. 1959. 9p. (U. S. Atomic Energy Commission. HW-61942)
62. Neidner, Robert, GEH-14-13, 14, 15, 16, 17, 18. PuO_2 impregnated graphite capsule irradiation. 1959. 5p. (U. S. Atomic Energy Commission. HW-60693)
63. Neidner, Robert. GEH-14-21, 22: low density UO_2 - PuO_2 capsule irradiation. 1959. 10p. (U. S. Atomic Energy Commission. HW-61939)
64. Neidner, Robert. GEH-14-23, 24, 25, and 26: Al-Pu alloy capsule irradiation. 1958. 2p. (U. S. Atomic Energy Commission. HW-57313)
65. Neidner, Robert. GEH-3-24. Pu-Al capsule irradiation. 1957. 7p. (U. S. Atomic Energy Commission. HW-48745)
66. Nertney, R. J. (ed.) Calculated surface temperatures for nuclear systems and analysis of their uncertainties. 1957. 73p. (U. S. Atomic Energy Commission. IDO-16343)
67. Richards, E. L. and E. A. Wright. A metallographic examination of zirconium and zirconium alloys. In: Bettis technical review. 1958. p.26-38. (U. S. Atomic Energy Commission. WAPD-BT-6)
68. Runnalls, O. J. C. Irradiation experience with rods of plutonium-aluminum alloy. In: International conference on the peaceful uses of atomic energy, Geneva, 1958. Proceedings. Vol. 6. Great Britain, United Nations Publication, 1958. p.710-717. (Paper p/191)
69. Sachs, George and Kent R. Van Horn. Practical Metallurgy. 7th ed. Cleveland, American Society for Metals, 1951. 567p.

70. Thomas, Ivor D. and Oswald J. Wick. Summary of aluminum-plutonium fuel development at Hanford. 1960. 25p. (France. Conference Internationale sur la Metallurgie Du Plutonium. Memoire no. 37)
71. Van Sice, R. B. (ed.) Hydraulic flow calculations for MTR-ETR experiments-standard practices manual. 1957. 69p. (U. S. Atomic Energy Commission. IDO-16368)
72. Voiland, Eugene E. Problems associated with the chemical processing of aluminum-silicon-plutonium fuel materials. 1958. 13p. (U. S. Atomic Energy Commission. HW-54819)
73. Waldron, M. B. et al. Plutonium technology for reactor systems. In: International conference on the peaceful uses of atomic energy, Geneva, 1958. Proceedings. Vol. 6. Great Britain, United Nations Publication, 1958. p.690-696. (Paper p/1452)
74. Weber, C. E. Progress on dispersion elements. In: Progress in nuclear energy. Vol. 2. Belfast, Pergamon Press, 1959. p.295-362. (ser. 5)
75. Wheeler, Robert G. Thermal conductance. 1957. 12p. (U. S. Atomic Energy Commission. HW-53598)
76. Wick, Oswald J. Quarterly reports of the plutonium Fuels Development, Plutonium Metallurgy Operation, General Electric Company, Hanford Atomic Products Operation, Richland, Washington.

HW-52035, October-December, 1956. 6p.

HW-51853, January-March, 1957. 21p.

HW-51854, April-June, 1957. 27p.

HW-54365, July-September, 1957. 36p.

HW-55415, October-December, 1957. 32p.

HW-57343, January-March, 1958. 25p.

HW-57342, April-June, 1958. 31p.

HW-59365, July-September, 1958. 26p.

HW-60996, October-December, 1958. 29p.

HW-61994, January-March, 1959. 42p.

April-June, 1959.

July-September, 1959.

October-December, 1960.

January-March, 1960.

1957-1960. (U. S. Atomic Energy Commission. HW-52035, 51853, 51854, 54365, 55415, 57343, 57342, 59365, 60996, 61994)



WATSON'S

PARCHMENT

LINEN

U.S.A.

BERKSHIRE

APPENDIX

100% COTTON FIBER



WATSON'S

ESTIMATE OF PRECISION
OF TABULAR VALUES

Item	Possible Error in Tabulated Value
(A) Alloy Capsules	
Pu Concentration	± 5% of value
Exposure	± 19% of value
Neutron Flux	± 19% of value
Fissions/cu cm	± 23% of value
Fractional Burnup	± 18% of value
$\Delta V/V$; by ΔD , ΔL	value ± 0.5
$\Delta V/V$; by Density	value ± 0.22
Length Change, ΔL	value ± 1.5×10^{-3} in.
Diameter Change, ΔD	value ± 1.0×10^{-3} in.
Burnup Analysis (Ce 147)	± 25% of value
(B) Alloy Clusters	
Pu Concentration	± 5% of value
Exposure	± 25% of value
$\Delta V/V$; by ΔD , ΔL	value ± 0.5
Length Change, ΔL	value ± 11×10^{-3} in.
Diameter Change, ΔD	value ± 1.0×10^{-3} in.
Burnup Analysis	± 25% of value
(C) Oxide Capsules	
Pu Concentration	value ± 0.0001
Density	value ± 0.5
Exposure	± 19% of value
Neutron Flux	± 19% of value
Gas Release	possibly ± 50% of value

NOTATION

<u>SYMBOL</u>	<u>DESCRIPTION</u>
Al-1.8 Pu	Aluminum - 1.8 weight percent plutonium alloy.
β^-	Negative beta particle
ETR	Engineering Test Reactor, Arco, Idaho
GEH-14-5	MTR irradiation test identification number. GEH-14 (originally GEH-3) means GEH-14 Facility and 5 means Capsule No. 5. Low pressure and temperature coolant present.
GEH-3-24-11	MTR irradiation test identification number. GEH-3 means GEH-3- Facility, 24 means Test No. 24, and 11 means Capsule No. 11. Low pressure and temperature coolant present.
IP186A	KER Loop Facility irradiation test identification number.
KER-Loop 1	Loop No. 1 of the KER Loop Facility at Hanford. The loops have high pressure and temperature coolant.
MTR	Materials Testing Reactor, Arco, Idaho
(n, γ)	(neutron, gamma) reaction
Zircaloy-2	Alloy of Zr with 1.25-1.65 % Sn, 0.07-0.17 % Fe, 0.06-0.14 % Cr, and 0.03-0.07 % Ni.
Zircaloy-3	Alloy of Zr with 0.20-0.30 % Sn and 0.20-0.30 % Fe.

<u>SYMBOL</u>	<u>DESCRIPTION</u>	<u>UNIT</u>
A_A	Annulus area	sq ft
a/o	Atomic percent	%
a, b, c	Constants in second order equation	- - -
bK	For the Modified Colburn Equation, b is the "base factor"(contains temperature dependent parameters) and K is the "K factor"(contains parameters based on physical dimensions)	Btu/(hr)(sq ft)(°F)

<u>SYMBOL</u>	<u>DESCRIPTION</u>	<u>UNIT</u>
c_p	Specific heat at constant pressure	Btu/(lb)(°F)
c_v	Specific heat at constant volume	Btu/(lb)(°F)
D	Diameter	in.
D_e	Effective diameter, for heat transfer or hydraulic case	ft
ΔL	Change in length	in.
Δp	Pressure drop	psig
Δt_c	Fuel core temperature drop	°F
Δt_f	Film temperature drop	°F
Δt_i	Interface temperature drop	°F
Δt_j	Jacket temperature drop	°F
ΔV	Change in volume	cu in.
f	Correction factor for departure from "1/v" law	- - -
f	Friction factor	- - -
f	Subscript - evaluate at film temperature	- - -
F.B.	Fractional burn-up of plutonium atoms	%
f(r)	Function of radius, r	nv
F _{ss}	Self-shielding factor	- - -
G	Mass flow	lb/(sec)(sq)(ft)
g_c	Gravitational constant	ft/(sec)(sec)
H_F	Maximum heat flux	Btu/(hr)(sq ft)
h_f	Film coefficient	Btu/(hr)(sq ft)(°F)

<u>SYMBOL</u>	<u>DESCRIPTION</u>	<u>UNIT</u>
h_i	Interface thermal conductance	Btu/(hr)(sq ft)(°F)
ID	Inside diameter	in.
k	Thermal conductivity	Btu/(hr)(ft)(°F)
k_{Al}	Thermal conductivity of aluminum	Btu/(hr)(ft)(°F)
k_{Al-Pu}	Thermal conductivity of Al-Pu alloy	Btu/(hr)(ft)(°F)
$k_{Al-Si-Pu}$	Thermal conductivity of Al-Si-Pu alloy	Btu/(hr)(ft)(°F)
k_f	$k_f = 3.204 \times 10^{-11}$ watt-sec/fission, if one assumes 200 mev/fission	(watt)(sec)/fission
(kT)	Average neutron energy in electron volts	ev
k_z	Mean thermal conductivity of Zircaloy	Btu/(hr)(ft)(°F)
l	Length of stringer basket	ft
mev	Million electron volts	10^6 ev
MWD/month	Output	(megawatt)(day)/month
MWD/T	Exposure	(megawatt)(day)/ton
μ	Viscosity, dynamic	lb/(hr)(ft)
N	Nuclear density of fissionable plutonium	atoms/(cu cm)
N_{Re}	Reynolds number	- - -
nvt	Integrated exposure, nvt = (nv)(sec)	neutrons/(sq cm)
OD	Outside diameter	in.
P	Vapor pressure	mm Hg
pH	Hydrogen ion concentration	- - -

<u>SYMBOL</u>	<u>DESCRIPTION</u>	<u>UNIT</u>
Pr	Prandtl number	- - -
ϕ	Thermal neutron flux, $\phi = nv = \left[\frac{\text{neutrons}}{\text{cu cm}} \right] \left[\frac{\text{cm}}{\text{sec}} \right]$	neutrons/(sq cm)(sec)
$\phi_{\text{avg}} = \phi$ average	Average thermal neutron flux over fuel core cross section	nv
$\phi_{\text{cc}} = \phi$ core center =	Thermal neutron flux at core center	nv
$\phi_{\text{CS}} = \phi$ core surface	Thermal neutron flux at fuel core surface	nv
ϕ_i	Thermal neutron flux at distance r_i from fuel core center	nv
$\phi_{\text{mod}} = \phi$ moderator	Thermal neutron flux in moderator	nv
Q_1	Specific power generation	kw/(ft of rod)
Q	Power generation	Btu/(hr)(ft of rod)
Q'''	Power generation, volumetric	kw/(cu in.)
q'''	Power generation, volumetric	watts/(cu cm)
r	Fuel core radius	cm
r_i	Radial distance from fuel core center to point i	cm
ρ	Density, actual	lb/(cu ft)
ρ_0	Density, theoretical	lb/(cu ft)
ρ_{alloy}	Density of alloy	gm/(cu cm)
ρ_{Al}	Density of aluminum	gm/(cu cm)
ρ_{Pu}	Density of plutonium	gm/(cu cm)
ρ_{PuAl_4}	Density of PuAl_4	gm/(cu cm)
$\bar{\sigma}_f$	Effective microscopic fission cross section	barns

<u>SYMBOL</u>	<u>DESCRIPTION</u>	<u>UNIT</u>
$\bar{\sigma}_a$	Effective microscopic absorption cross section	barns
Σ_f	Macroscopic fission cross section, $\Sigma_f = N \bar{\sigma}_f^{Pu}$	1/cm
$\bar{\sigma}_f^{Pu}$	Microscopic fission cross section for plutonium	barns
$\sigma(kT)$	Monoenergetic cross section at the temperature, T, associated with the most probable energy of a Maxwell distribution	barns
t	Temperature, Centigrade	°C
t	Temperature, Fahrenheit	°F
T _o	Temperature, Kelvin (for t = 20°C)	°K
T	Temperature, Kelvin	°F
t _f	Film temperature, t _f , equals t _w plus $\frac{1}{2} (\Delta t_f)$	°F
t _{max}	Maximum fuel core temperature	°F
t _s	Fuel core surface temperature	°F
t _w	Coolant bulk water temperature	°F
v	Volume of core material	(cu cm)/(ft of rod)
V	Velocity	ft/sec
V	Volume	cu in.
$\Delta v/v$	Volume increase	%